

Projected exponential methods for stiff dynamical low-rank approximation problems

Benjamin Carrel^{1*} and Bart Vandereycken¹

^{1*}Mathematics, University of Geneva, Rue du Conseil-Général, Geneva, 1205, Switzerland.

*Corresponding author(s). E-mail(s): benjamin.carrel@unige.ch;
Contributing authors: bart.vandereycken@unige.ch;

Abstract

The numerical integration of stiff equations is a challenging problem that needs to be approached by specialized numerical methods. Exponential integrators form a popular class of such methods since they are provably robust to stiffness and have been successfully applied to a variety of problems. The dynamical low-rank approximation is a recent technique for solving high-dimensional differential equations by means of low-rank approximations. However, the domain is lacking numerical methods for stiff equations since existing methods are either not robust-to-stiffness or have unreasonably large hidden constants.

In this paper, we focus on solving large-scale stiff matrix differential equations with a Sylvester-like structure, that admit good low-rank approximations. We propose two new methods that have good convergence properties, small memory footprint and that are fast to compute. The theoretical analysis shows that the new methods have order one and two, respectively. We also propose a practical implementation based on Krylov techniques. The approximation error is analyzed, leading to a priori error bounds and, therefore, a mean for choosing the size of the Krylov space. Numerical experiments are performed on several examples, confirming the theory and showing good speedup in comparison to existing techniques.

Keywords: dynamical low-rank approximation, exponential methods, projection methods, Krylov methods, Sylvester differential equations, stiff equations

MSC Classification: 65F55 , 65F60 , 65L04 , 65L05 , 65L70

1 Introduction

In this work, we are interested in the numerical integration of large-scale and stiff initial value problems. A stiff problem is a problem for which an implicit method, like implicit Euler, is significantly faster than its explicit counterpart, like explicit Euler. Since stiffness is intrinsic to the problem, it cannot be avoided by reformulation and needs to be integrated by specialized numerical methods. The archetypal example is the heat equation $\partial_t u = \Delta u + g(u)$.

We consider discretized partial differential equations (PDEs), where the stiff components have been approximated by linearization, leading to a Sylvester-like differential equation

$$\dot{X}(t) = AX(t) + X(t)B + \mathcal{G}(t, X(t)), \quad X(0) = X_0 \in \mathbb{R}^{m \times n}.$$

The time independent matrices $A \in \mathbb{R}^{m \times m}$ and $B \in \mathbb{R}^{n \times n}$ are typically very large but also sparse or structured. When we are dealing with such large-scale problems, we cannot afford to store nor compute

the dense solution $X(t)$. We therefore need some kind of data sparse representation for $X(t)$, like low-rank approximations. Applications of such large Sylvester-like differential equations arise in various fields, including numerical simulations, control theory, signal processing; see also Section 5 and references therein for examples and more details.

The dynamical low-rank approximation (DLRA) [1] is a popular technique that allows to compute an approximation of the solution by a low-rank matrix: $Y(t) \approx X(t)$ such that $\text{rank}(Y(t)) = r \ll m, n$. The technique has been successfully applied in various areas, including control theory, signal processing, machine learning, image compression, and quantum physics. The projector-splitting integrator [2] as well as the so-called unconventional integrator [3] are two efficient integrators of the DLRA, but the current convergence bounds [4] rely on the Lipschitz constant of the vector field, making these methods theoretically and practically not suitable for stiff problems.

The key idea of exponential methods [5] is to solve exactly the stiff part of the ODE. These methods are robust to stiffness by construction and their theoretical properties are well studied. In the same spirit, a low-rank Lie–Trotter splitting [6] is shown to be robust to stiffness and can be used to solve the DLRA for parabolic problems. However, the Lie–Trotter and Strang splittings employed there suffer from large hidden constants in their error estimates, making the methods unfortunately unpractical.

In this paper, we propose a new class of methods that we call projected exponential methods. These methods are robust to stiffness, have small hidden constants in the error estimates, and the computations preserve the low-rank structure of the solution. The growth in rank of the sub-steps is contained by means of projections and Krylov iterative methods.

2 Notations and preliminaries

Let $A \in \mathbb{R}^{m \times m}$ and $B \in \mathbb{R}^{n \times n}$ be two matrices which lead to the stiffness¹. One can think of these matrices as discretized operators obtained from a particular PDE. Under mesh refinement, their Lipschitz constants will grow in an unbounded way, causing stiffness. In this work, we are interested in solving general Sylvester-like differential equations of the form

$$\begin{aligned} \dot{X}(t) &= AX(t) + X(t)B + \mathcal{G}(X(t)), \quad t \in [0, T] \\ X(0) &= X_0 \in \mathbb{R}^{m \times n}, \end{aligned} \tag{1}$$

where $\mathcal{G}: \mathbb{R}^{m \times n} \rightarrow \mathbb{R}^{m \times n}$ is a non-linear but non-stiff² operator. For ease of notation, we will often denote the linear Sylvester operator as \mathcal{L} , defined by $\mathcal{L}X = AX + XB$. Throughout, we will denote $f(t) = \mathcal{G}(X(t))$ and assume that $f(t)$ is absolutely continuous on the compact domain of integration $[0, T]$. It is sometimes assumed to be higher-order differentiable when needed. Without loss of generality, equation (1) is autonomous. Occasionally, we will denote the full vector field $\mathcal{F} = \mathcal{L} + \mathcal{G}$. Whenever we use calligraphic notation for an operator, it has to be interpreted as acting on the matrix: $\mathcal{L}X = \mathcal{L}(X)$ is not (in general) the matrix multiplication of \mathcal{L} and X but the linear operator \mathcal{L} applied to the matrix X . The same holds for matrix functions, like $e^{t\mathcal{L}}$ in the next lemma.

Lemma 1 (Closed-form solution). *The solution to the initial value problem*

$$\dot{X}(t) = \mathcal{L}X(t) + \mathcal{G}(X(t)), \quad X(0) = X_0,$$

is given by the closed-form formula

$$X(t) = e^{t\mathcal{L}}X_0 + \int_0^t e^{(t-s)\mathcal{L}}\mathcal{G}(X(s))ds. \tag{2}$$

The following definitions will be useful in the analysis of the methods. Throughout, we will denote by $\|\cdot\|$ the Frobenius norm, which is induced by the Euclidean inner product $\langle \cdot, \cdot \rangle$. Other norms will be specified explicitly.

¹In this work, we call a method robust to stiffness if it does not depend on the Lipschitz constant of the stiff part of the vector field. It may however depend on the one-sided Lipschitz constant.

²By non-stiff, we mean that the Lipschitz constant of \mathcal{G} remains bounded under mesh refinement. In practice, it should also not be too large.

Definition 1 (One-sided Lipschitz). Let $\mathcal{F}: \mathbb{R}^{m \times n} \rightarrow \mathbb{R}^{m \times n}$ be an operator, not necessarily linear. Its one-sided Lipschitz constant $\ell_{\mathcal{F}}$ is the smallest constant such that

$$\langle X - Y, \mathcal{F}(X) - \mathcal{F}(Y) \rangle \leq \ell_{\mathcal{F}} \|X - Y\|^2 \quad \forall X, Y \in \mathbb{R}^{m \times n}. \quad (3)$$

For linear operators, like \mathcal{L} , the one-sided Lipschitz constant can be calculated explicitly. In particular, condition (3) is equivalent to

$$\ell_{\mathcal{L}} = \max_{X-Y \neq 0} \frac{\langle X - Y, \mathcal{L}(X - Y) \rangle}{\|X - Y\|^2} = \max_{W \neq 0} \frac{\langle W, \mathcal{L}W \rangle}{\|W\|^2}.$$

Since \mathcal{L} is defined³ on \mathbb{R} , we have $\langle W, \mathcal{L}W \rangle = \langle W, \mathcal{L}^*W \rangle$ with \mathcal{L}^* the adjoint of \mathcal{L} . This allow us to write the one-sided Lipschitz constant as the maximal value of the Rayleigh quotient of a symmetric matrix, which is attained by the maximal eigenvalue of this matrix:

$$\ell_{\mathcal{L}} = \frac{1}{2} \max_{W \neq 0} \frac{\langle W, (\mathcal{L} + \mathcal{L}^*)W \rangle}{\|W\|^2} = \frac{1}{2} \lambda_{\max}(\mathcal{L} + \mathcal{L}^*).$$

The above formula is valid for any linear \mathcal{L} . In case, $\mathcal{L}(X) = AX + XB$ is the Sylvester operator, we can go one step further and obtain

$$\ell_{\mathcal{L}} = \frac{1}{2} \lambda_{\max}(A + A^*) + \frac{1}{2} \lambda_{\max}(B + B^*).$$

This follows from the matrix representation of \mathcal{L} as $I \otimes A + B^T \otimes I$ and properties of the Kronecker product; see, e.g., [7, Chap. 4.4].

Definition 2 (Lipschitz continuity). An operator $\mathcal{F}: \mathbb{R}^{m \times n} \rightarrow \mathbb{R}^{m \times n}$ is locally Lipschitz-continuous in a strip along the exact solution X of (1) if there exists $R > 0$ and $L_{\mathcal{F}} \in \mathbb{R}$ such that, for all $t \in [0, T]$,

$$\|\mathcal{F}(Y(t)) - \mathcal{F}(Z(t))\| \leq L_{\mathcal{F}} \|Y(t) - Z(t)\|,$$

if $\|X(t) - Y(t)\| \leq R$ and $\|X(t) - Z(t)\| \leq R$.

Remark 1. By elementary properties of the one-sided and the standard Lipschitz constants, we have for $\mathcal{F} = \mathcal{L} + \mathcal{G}$ that

$$\ell_{\mathcal{F}} \leq \ell_{\mathcal{L}} + \ell_{\mathcal{G}} \leq \ell_{\mathcal{L}} + L_{\mathcal{G}}.$$

For diffusive problems, $\ell_{\mathcal{L}}$ can be negative. As we will see, obtaining error bounds in terms of one-sided Lipschitz constants can therefore be very beneficial in this case, even when $L_{\mathcal{G}}$ is always positive.

For completeness, we briefly introduce φ -functions which are central in the analysis and implementation of exponential integrators.

Definition 3 (φ -functions [8]). Let $\mathcal{L}: \mathbb{R}^{m \times n} \rightarrow \mathbb{R}^{m \times n}$ be a linear operator. The φ -functions are defined as

$$\begin{aligned} \varphi_0(t\mathcal{L}) &= e^{t\mathcal{L}}, \\ \varphi_k(t\mathcal{L}) &= \frac{1}{t^k} \int_0^t e^{(t-s)\mathcal{L}} \frac{s^{k-1}}{(k-1)!} ds, \quad k \geq 1. \end{aligned}$$

A number of equivalent definitions exist for φ -functions. We first mention

$$\varphi_k(z) = \frac{e^z - p_{k-1}(z)}{z^k}, \quad p_{k-1}(z) = \sum_{j=0}^{k-1} \frac{z^j}{j!}, \quad (4)$$

for scalar values $z \neq 0$ which is useful for explicit calculations with Taylor series. Next, the following definition makes the link with ODEs clear.

³While we focus on \mathbb{R} , the following derivations are similar in \mathbb{C} .

Lemma 2 (φ -functions as IVPs [8, 9]). Let $Z_i \in \mathbb{R}^{m \times n}$ for $i = 0, \dots, n$. The φ -functions are equivalently defined by the differential equations

$$\begin{aligned} Z(t) = \varphi_0(t\mathcal{L})Z_0 &\iff \dot{Z}(t) = \mathcal{L}Z(t), \quad Z(0) = Z_0, \\ Z(t) = t^k \varphi_k(t\mathcal{L})Z_k &\iff \dot{Z}(t) = \mathcal{L}Z(t) + \frac{t^{k-1}}{(k-1)!}Z_k, \quad Z(0) = 0. \end{aligned}$$

By linearity, we have that

$$Z(t) = e^{t\mathcal{L}}Z_0 + \sum_{k=1}^n t^k \varphi_k(t\mathcal{L})Z_k \iff \dot{Z}(t) = \mathcal{L}Z(t) + \sum_{k=1}^n \frac{t^{k-1}}{(k-1)!}Z_k, \quad Z(0) = Z_0.$$

Bounding these φ -functions appropriately is crucial for the analysis of exponential integrators introduced in the next section. The derivation of such bounds requires to use the logarithmic norm (which, despite the name, is not a norm).

Definition 4 (Logarithmic norm). The logarithmic norm of a linear operator $\mathcal{L}: \mathbb{R}^{m \times n} \rightarrow \mathbb{R}^{m \times n}$ is defined as

$$\mu_{\mathcal{L}} = \lim_{h \rightarrow 0^+} \frac{\|I + h\mathcal{L}\|_2 - 1}{h},$$

where $\|\cdot\|_2$ is the spectral norm.

It is well known (see, e.g., [10, Thm. I.10.5]) that the logarithmic norm for the spectral norm satisfies

$$\mu_{\mathcal{L}} = \frac{1}{2} \lambda_{\max}(\mathcal{L} + \mathcal{L}^*).$$

This implies $\mu_{\mathcal{L}} = \ell_{\mathcal{L}}$, the logarithmic norm equals the one-sided Lipschitz constant for a linear operator \mathcal{L} . From now on, we will only use the notation $\ell = \ell_{\mathcal{L}}$, and specify the index when needed.

Lemma 3 (φ -functions are bounded). For any matrix $X \in \mathbb{R}^{m \times n}$, we have for all $k = 0, 1, \dots$ that

$$\|\varphi_k(h\mathcal{L})X\|_{\star} \leq \varphi_k(h\ell_{\mathcal{L}}) \|X\|_{\star}, \quad h \geq 0,$$

where $\|\cdot\|_{\star}$ is either the spectral norm $\|\cdot\|_2$ or the Frobenius norm $\|\cdot\|$.

Proof. Consider the differential equation $\dot{Z}(t) = \mathcal{L}Z(t) + R(t)$, where $R(t) \in \mathcal{C}^2$ is specified below. Denote $\ell = \ell_{\mathcal{L}}$. Then, by definition of the Dini derivative, we have

$$\begin{aligned} D_t^+ \|Z(t)\|_{\star} &= \limsup_{h \rightarrow 0^+} \frac{\|Z(t+h)\|_{\star} - \|Z(t)\|_{\star}}{h} \\ &= \lim_{h \rightarrow 0^+} \frac{\|Z(t) + h\mathcal{L}Z(t) + hR(t)\|_{\star} - \|Z(t)\|_{\star}}{h} \\ &\leq \lim_{h \rightarrow 0^+} \frac{\|Z(t) + h\mathcal{L}Z(t)\|_{\star} - \|Z(t)\|_{\star}}{h} + \|R(t)\|_{\star} \\ &\leq \lim_{h \rightarrow 0^+} \frac{\|I + h\mathcal{L}\|_2 - 1}{h} \|Z(t)\|_{\star} + \|R(t)\|_{\star} \\ &= \ell \|Z(t)\|_{\star} + \|R(t)\|_{\star}, \end{aligned}$$

since $\|\cdot\|_{\star}$ is sub-multiplicative. The solution of this Dini differential equation verifies (see, e.g., [10, Theorem 10.1])

$$\|Z(t)\|_{\star} \leq e^{t\ell} \|Z(0)\|_{\star} + \int_0^t e^{(t-\tau)\ell} \|R(\tau)\|_{\star} d\tau.$$

From Lemma 2 with $t = h$, the claimed inequality for $k = 0$ is obtained with $Z(0) = X$ and $R(t) = 0$. For $k \geq 1$, we take $Z(0) = 0$ and $R(t) = \frac{t^{k-1}}{(k-1)!}X$ which gives $Z(t) = t^k \varphi_k(t\mathcal{L})X$ by the same Lemma. The inequality above reduces to

$$\|Z(t)\|_{\star} \leq \int_0^t e^{(t-\tau)\ell} \frac{\tau^{k-1}}{(k-1)!} d\tau \|X\|_{\star} = t^k \varphi_k(t\ell) \|X\|_{\star}.$$

Combining gives the desired result. \square

2.1 Exponential integrators

Exponential integrators are a particular class of integrators well suited for parabolic partial differential equations (PDEs). In this paper, the analysis is restricted to matrix differential equations even though the analysis and the application of exponential integrators apply to a larger class of differential equations in Banach spaces. While we start by rephrasing some results from [11] and [5], we later derive new results specialized to our framework and necessary for the analysis of the new methods.

Exponential Euler

Let $h > 0$ be a time step and define $X_0^E = X_0$. Interpolating the integral in (2) at the initial value leads to the so-called *exponential Euler* method, which iterates

$$X_{n+1}^E = e^{h\mathcal{L}} X_n^E + h\varphi_1(h\mathcal{L}) \mathcal{G}(X_n^E). \quad (5)$$

According to the stability conditions (7) discussed below, this method is also the only sensible choice for a one-stage method. In the context of matrices, its analysis is straightforward and the following theorem states its convergence behavior. It can be proven like the related result for exponential Runge method below; we refer to Appendix A for a self-contained proof.

Theorem 4 (Convergence of exponential Euler). *Assume that \mathcal{G} is locally Lipschitz-continuous in a strip along the exact solution. Let X_n^E be the n -th iteration of the exponential Euler scheme (5), and let $X(t_n)$ be the solution to (1) at time $t_n = nh$. Then, for all $h \leq h_0$, the error verifies*

$$\|X_n^E - X(t_n)\| \leq C \cdot h \cdot \max_{0 \leq t \leq t_n} \left\| \frac{d}{dt} \mathcal{G}(X(t)) \right\|,$$

where the constant C is explicitly available in the proof and depends on ℓ, L_G, h_0 and t_n but not on the step-size h nor the number of iterations n .

The method is therefore order one in h and robust to stiffness since the hidden constant does not depend on the Lipschitz constant of the stiff operator \mathcal{L} . The proof is given in Appendix A; it is similar to the proof of the two-stage method stated below but easier. The hidden constant is relatively small (and even often $C \leq 1$) for reasonable values of $L_G > 0$ and $\ell < 0$.

Exponential Runge–Kutta

The methods are motivated by the closed form solution (2) on which we apply quadrature formulas. The so-called *exponential Runge–Kutta* methods with s stages are given by

$$\begin{aligned} G_{nj} &= \mathcal{G}(X_{nj}), & \text{for } j = 1, \dots, s \\ X_{ni} &= e^{c_i h \mathcal{L}} X_n + h \sum_{j=1}^s a_{ij}(h\mathcal{L}) G_{nj}, & \text{for } i = 1, \dots, s \\ X_{n+1} &= e^{h\mathcal{L}} X_n + h \sum_{i=1}^s b_i(h\mathcal{L}) G_{ni}. \end{aligned} \quad (6)$$

The choice of operators $a_{ij}(h\mathcal{L}), b_i(h\mathcal{L})$, and coefficients c_i , plays a crucial role in the behavior of the resulting method. In the next paragraphs, we derive explicit order conditions and then focus on the two-stage methods.

Explicit stiff order conditions

A Runge–Kutta method is called explicit when $a_{ij} = 0$ for all $j > i - 1$. In the following, we discuss explicit order conditions leading to robust-to-stiffness methods. As introduced in [11], the first condition comes naturally by imposing the scheme to preserve the equilibria X^* of the autonomous problem

$\dot{X}(t) = \mathcal{L}X(t) + \mathcal{G}(X(t))$. Assuming the scheme starts in an equilibrium, we must have $X^* = X_n = X_{ni}$ for all $n > 0$ and $i \leq s$. Writing down the equations, we get the equilibrium conditions

$$\sum_{i=1}^s b_i(h\mathcal{L}) = \varphi_1(h\mathcal{L}), \quad \sum_{j=1}^{i-1} a_{ij}(h\mathcal{L}) = c_i\varphi_1(c_ih\mathcal{L}), \quad 1 \leq i \leq s. \quad (7)$$

The derivation of order conditions is well-known in the literature and is done for general operators in [11], [5] and also for higher-orders in [12] and then simplified in [13]. Such analysis requires that the expressions $\varphi_k(h\mathcal{L})$ are bounded, which we have shown in Lemma 3.

In the papers mentioned above, the analysis is typically done in a general Banach space, and the hidden constant are not given explicitly. Here, we do a similar analysis applied to finite dimensional vector spaces, which allows us to give explicit hidden constants, and therefore a better a priori control on the error. In particular, equation (15) below is not available as such in [11] but is needed in Lemma 5 and for the rest of our analysis.

Let us start by defining the errors

$$E_{ni} = X_{ni} - X(t_n + c_ih), \quad E_{n+1} = X_{n+1} - X(t_{n+1}). \quad (8)$$

In the following, we are going to perform a Taylor expansion on the function $f(t) = \mathcal{G}(X(t))$, where $X(t)$ is the solution to the full problem (1). We therefore assume that \mathcal{G} is sufficiently differentiable. Then, we plug the expansion in the definition of the method (6) and compare with the closed form formula:

$$X(t_n + \theta h) = e^{\theta h\mathcal{L}}X(t_n) + \int_0^{\theta h} e^{(\theta h - \tau)\mathcal{L}}f(t_n + \tau)d\tau. \quad (9)$$

Assuming \mathcal{G} sufficiently differentiable, a Taylor expansion gives

$$f(t_n + \tau) = \sum_{j=1}^q \frac{\tau^{j-1}}{(j-1)!} f^{(j-1)}(t_n) + \int_0^\tau \frac{(\tau - \sigma)^{q-1}}{(q-1)!} f^{(q)}(t_n + \sigma)d\sigma, \quad (10)$$

and therefore we have with (3) that

$$X(t_n + c_ih) = e^{c_ih\mathcal{L}}X(t_n) + \sum_{j=1}^{q_i} (c_ih)^j \varphi_j(c_ih\mathcal{L}) f^{(j-1)}(t_n) + \int_0^{c_ih} e^{(c_ih - \tau)\mathcal{L}} \int_0^\tau \frac{(\tau - \sigma)^{q_i-1}}{(q_i-1)!} f^{(q_i)}(t_n + \sigma)d\sigma d\tau. \quad (11)$$

Next, the exact solution agrees with the numerical schemes up to the defects:

$$\begin{aligned} X(t_n + c_ih) &= e^{c_ih\mathcal{L}}X(t_n) + h \sum_{j=1}^{i-1} a_{ij}(h\mathcal{L}) f(t_n + c_jh) + \Delta_{ni}, \\ X(t_{n+1}) &= e^{h\mathcal{L}}X(t_n) + h \sum_{i=1}^s b_i(h\mathcal{L}) f(t_n + c_ih) + \delta_{n+1}. \end{aligned} \quad (12)$$

Now using again the Taylor expansion (10), we get

$$\begin{aligned} X(t_n + c_ih) &= e^{c_ih\mathcal{L}}X(t_n) + h \sum_{j=1}^{i-1} a_{ij}(h\mathcal{L}) \left(\sum_{k=1}^{q_i} \frac{(c_jh)^{k-1}}{(k-1)!} f^{(k-1)}(t_n) + \int_0^{c_jh} \frac{(c_jh - \sigma)^{q_i-1}}{(q_i-1)!} f^{(q_i)}(t_n + \sigma)d\sigma \right) + \Delta_{ni}, \\ X(t_{n+1}) &= e^{h\mathcal{L}}X(t_n) + h \sum_{i=1}^s b_i(h\mathcal{L}) \left(\sum_{k=1}^q \frac{(c_ih)^{k-1}}{(k-1)!} f^{(k-1)}(t_n) + \int_0^{c_ih} \frac{(c_ih - \sigma)^{q-1}}{(q-1)!} f^{(q)}(t_n + \sigma)d\sigma \right) + \delta_{n+1}. \end{aligned} \quad (13)$$

Comparing equations (11) and (13) gives the following expressions for the defects:

$$\begin{aligned}\Delta_{ni} &= \sum_{j=1}^{q_i} h^j \psi_{j,i}(h\mathcal{L}) f^{(j-1)}(t_n) + \Delta_{ni}^{[q_i]}, & \psi_{j,i}(h\mathcal{L}) &= \varphi_j(c_i h\mathcal{L}) c_i^j - \sum_{k=1}^{i-1} a_{ik}(h\mathcal{L}) \frac{c_k^{j-1}}{(j-1)!}, \\ \delta_{n+1} &= \sum_{j=1}^q h^j \psi_j(h\mathcal{L}) f^{(j-1)}(t_n) + \delta_{n+1}^{[q]}, & \psi_j(h\mathcal{L}) &= \varphi_j(h\mathcal{L}) - \sum_{k=1}^s b_k(h\mathcal{L}) \frac{c_k^{j-1}}{(j-1)!},\end{aligned}\tag{14}$$

and the remainders are explicitly given by

$$\begin{aligned}\Delta_{ni}^{[q_i]} &= \int_0^{c_i h} e^{(c_i h - \tau)\mathcal{L}} \int_0^\tau \frac{(\tau - \sigma)^{q_i - 1}}{(q_i - 1)!} f^{(q_i)}(t_n + \sigma) d\sigma d\tau - h \sum_{j=1}^{i-1} a_{ij}(h\mathcal{L}) \int_0^{c_j h} \frac{(c_j h - \sigma)^{q_i - 1}}{(q_i - 1)!} f^{(q_i)}(t_n + \sigma) d\sigma, \\ \delta_{n+1}^{[q]} &= \int_0^h e^{(h - \tau)\mathcal{L}} \int_0^\tau \frac{(\tau - \sigma)^{q-1}}{(q-1)!} f^{(q)}(t_n + \sigma) d\sigma d\tau - h \sum_{i=1}^s b_i(h\mathcal{L}) \int_0^{c_i h} \frac{(c_i h - \sigma)^{q-1}}{(q-1)!} f^{(q)}(t_n + \sigma) d\sigma.\end{aligned}\tag{15}$$

Finally, the general recursion for the errors (8) is given by

$$\begin{aligned}E_{ni} &= e^{c_i h\mathcal{L}} E_n + h \sum_{j=1}^{i-1} a_{ij}(h\mathcal{L}) [\mathcal{G}(X_{nj}) - f(t_n + c_j h)] - \Delta_{ni}, \\ E_{n+1} &= e^{h\mathcal{L}} E_n + h \sum_{i=1}^s b_i(h\mathcal{L}) [\mathcal{G}(X_{ni}) - f(t_n + c_i h)] - \delta_{n+1}.\end{aligned}\tag{16}$$

Except for equation (15), the derivations above are not new and are also derived in [11], where the analysis is then performed directly on the recursion of the error. The new methods, however, require a different approach because of the truncation operators as we will see in Section 3. We therefore need the following lemma from which we will derive our own analysis.

Lemma 5. *Assume that $f(t) = \mathcal{G}(X(t))$ is sufficiently differentiable. For all $h \leq h_0$, the remainders given in (15) are bounded by*

$$\begin{aligned}\left\| \Delta_{ni}^{[q_i]} \right\| &\leq C_i^{[q_i]} \cdot h^{q_i+1} \cdot \max_{0 \leq s \leq h} \left\| f^{(q_i)}(t_n + s) \right\|, \\ \left\| \delta_{n+1}^{[q]} \right\| &\leq C^{[q]} \cdot h^{q+1} \cdot \max_{0 \leq s \leq h} \left\| f^{(q)}(t_n + s) \right\|.\end{aligned}$$

The constants depend on ℓ , the coefficients c_i and h_0 , but not on the number of steps n . They are explicitly available in the proof and we have, for example for the two-stage method (19), that

$$C_1^{[1]} = 0, \quad C_2^{[1]} = (c_2 h)^2 \varphi_2(h\ell), \quad C^{[2]} = h^3 \varphi_3(h\ell) + \frac{c_2^2 h^3}{2} \varphi_2(h\ell).$$

Proof. The proof is by direct calculations. For the remainder $\Delta_{ni}^{[q_i]}$:

$$\begin{aligned}\left\| \int_0^{c_i h} e^{(c_i h - \tau)\mathcal{L}} \int_0^\tau \frac{(\tau - \sigma)^{q_i - 1}}{(q_i - 1)!} f^{(q_i)}(t_n + \sigma) d\sigma d\tau \right\| &\leq \int_0^{c_i h} e^{(c_i h - \tau)\ell} \int_0^\tau \frac{(\tau - \sigma)^{q_i - 1}}{(q_i - 1)!} d\sigma d\tau \max_{0 \leq s \leq h} \left\| f^{(q_i)}(t_n + s) \right\| \\ &= (c_i h)^{q_i+1} \varphi_{q_i+1}(h\ell) \cdot \max_{0 \leq s \leq h} \left\| f^{(q_i)}(t_n + s) \right\|, \\ \left\| h \sum_{j=1}^{i-1} a_{ij}(h\mathcal{L}) \int_0^{c_j h} \frac{(c_j h - \sigma)^{q_i - 1}}{(q_i - 1)!} f^{(q_i)}(t_n + \sigma) d\sigma \right\| &\leq h \left\| \sum_{j=1}^{i-1} a_{ij}(h\mathcal{L}) \right\| \int_0^h \frac{(h - \sigma)^{q_i - 1}}{(q_i - 1)!} d\sigma \max_{0 \leq s \leq h} \left\| f^{(q_i)}(t_n + s) \right\| \\ &\leq h^{q_i+1} \cdot \frac{c_i \varphi_1(c_i h\ell)}{q_i!} \cdot \max_{0 \leq s \leq h} \left\| f^{(q_i)}(t_n + s) \right\|.\end{aligned}$$

In the second bound, we used the stability condition $\sum_{j=1}^{i-1} a_{ij}(h\mathcal{L}) = c_i \varphi_1(c_i h\mathcal{L})$. Therefore, the remainder is bounded by

$$\left\| \Delta_{ni}^{[q_i]} \right\| \leq C h^{q_i+1} \max_{0 \leq s \leq h} \left\| f^{(q_i)}(t_n + s) \right\|,$$

for some constant C independent of h , when $h \leq h_0$. The remainder $\delta_{n+1}^{[q]}$ is bounded similarly:

$$\begin{aligned} \left\| \int_0^h e^{(h-\tau)\mathcal{L}} \int_0^\tau \frac{(\tau-\sigma)^{q-1}}{(q-1)!} f^{(q)}(t_n + \sigma) d\sigma d\tau \right\| &\leq \int_0^h e^{(h-\tau)\ell} \int_0^\tau \frac{(\tau-\sigma)^{q-1}}{(q-1)!} d\sigma d\tau \cdot \max_{0 \leq s \leq h} \left\| f^{(q)}(t_n + s) \right\|, \\ &= h^{q+1} \varphi_{q+1}(h\ell) \cdot \max_{0 \leq s \leq h} \left\| f^{(q)}(t_n + s) \right\| \\ \left\| h \sum_{i=1}^s b_i(h\mathcal{L}) \int_0^{c_i h} \frac{(c_i h - \sigma)^{q-1}}{(q-1)!} f^{(q)}(t_n + \sigma) d\sigma \right\| &\leq h^{q+1} \cdot \frac{\varphi_1(h\ell)}{q!} \cdot \max_{0 \leq s \leq h} \left\| f^{(q)}(t_n + s) \right\|, \end{aligned}$$

where we used the stability condition $\sum_{i=1}^s b_i(h\mathcal{L}) = \varphi_1(h\mathcal{L})$. The conclusion follows immediately. \square

The order conditions are naturally obtained in expression (14) by imposing $\psi_{ij} = 0$ and $\psi_k = 0$ for all indexes i, j, k .

Exponential Runge

The second order conditions are obtained by imposing

$$\psi_{1,2}(h\mathcal{L}) \stackrel{!}{=} 0, \quad \text{and} \quad \psi_1(h\mathcal{L}) \stackrel{!}{=} 0 \stackrel{!}{=} \psi_2(h\mathcal{L}). \quad (17)$$

Combining with the equilibrium conditions (7), we obtain the following family of explicit methods for $c_2 \neq 0$, called the exponential Runge methods, in a Butcher table:

$$\begin{array}{c|c} 0 & \\ \hline c_2 & c_2 \varphi_{1,2} \\ \hline \varphi_1 - \frac{1}{c_2} \varphi_2 & \frac{1}{c_2} \varphi_2 \end{array} \quad (18)$$

Written more explicitly, this gives us the two-stage method

$$\begin{cases} X_{n2}^R = e^{c_2 h\mathcal{L}} X_n^R + c_2 h \varphi_1(c_2 h\mathcal{L}) \mathcal{G}(X_n^R), \\ X_{n+1}^R = e^{h\mathcal{L}} X_n^R + h \varphi_1(h\mathcal{L}) \mathcal{G}(X_n^R) + h \varphi_2(h\mathcal{L}) (\mathcal{G}(X_{n2}^R) - \mathcal{G}(X_n^R)). \end{cases} \quad (19)$$

The following theorem proves the convergence of these methods, and its proof gives information on the hidden constants.

Theorem 6 (Convergence of exponential Runge). *Assume that \mathcal{G} is locally Lipschitz-continuous in a strip along the exact solution, and sufficiently differentiable. Let X_n^R be the n -th iteration of the exponential Runge scheme (19) started at $X_0 = X(0)$, and let $X(t_n)$ be the solution to (1) at time $t_n = nh$. Then, for all $h \leq h_0$, the error verifies*

$$\|X_n^R - X(t_n)\| \leq C \cdot h^2 \cdot \left(\max_{0 \leq t \leq t_n} \left\| \frac{d}{dt} \mathcal{G}(X(t)) \right\| + \max_{0 \leq t \leq t_n} \left\| \frac{d^2}{dt^2} \mathcal{G}(X(t)) \right\| \right),$$

where the constant C depends on $\ell, L_{\mathcal{G}}, h_0$ and t_n but not on h nor n .

Proof. From (16) and taking the norm, the error verifies

$$\begin{aligned} \|E_{n+1}\| &= \left\| e^{h\mathcal{L}} E_n + h \sum_{i=1}^2 b_i(h\mathcal{L}) [\mathcal{G}(X_{ni}) - f(t_n + c_i h)] + \delta_{n+1} \right\| \\ &\leq e^{h\ell} \|E_n\| + h \sum_{i=1}^2 \|b_i(h\mathcal{L})\| \cdot L_{\mathcal{G}} \|E_{ni}\| + \|\delta_{n+1}\|. \end{aligned} \quad (20)$$

By definition of the exponential Runge method, we have that

$$\|E_{n1}\| = \|E_n\| + \|\Delta_{n1}\|, \quad \|E_{n2}\| \leq e^{c_2 h \ell} \|E_n\| + c_2 h \varphi_1(c_2 h \ell) \|E_{n1}\| + \|\Delta_{n2}\|,$$

and from the order conditions (17) and Lemma 5, it follows that

$$\begin{aligned} \|\Delta_{n1}\| &= \|\Delta_{n1}^{[1]}\| = 0, \quad \|\Delta_{n2}\| = \|\Delta_{n2}^{[1]}\| \leq (c_2 h)^2 \varphi_2(h\ell) \cdot \max_{0 \leq s \leq h} \|f'(t_n + s)\|, \\ \text{and } \|\delta_{n+1}\| &= \|\delta_{n+1}^{[2]}\| \leq \left[h^3 \varphi_3(h\ell) + \frac{c_2^2 h^3}{2} \varphi_2(h\ell) \right] \cdot \max_{0 \leq s \leq h} \|f''(t_n + s)\|. \end{aligned} \quad (21)$$

Next, we define the following quantities:

$$\beta_1 = (c_2 h)^2 \varphi_2(h\ell) \cdot \max_{0 \leq s \leq t_{n+1}} \|f'(s)\|, \quad \beta_2 = \left[h^2 \varphi_3(h\ell) + \frac{c_2^2 h^2}{2} \varphi_2(h\ell) \right] \cdot \max_{0 \leq s \leq t_{n+1}} \|f''(s)\|. \quad (22)$$

When $h \leq h_0 \leq c_2$, direct computations give that

$$\|b_1(h\mathcal{L})\| \leq \varphi_1(h\ell) - \frac{1}{c_2} \varphi_2(h\ell), \quad \|b_2(h\mathcal{L})\| \leq \frac{1}{c_2} \varphi_2(h\ell). \quad (23)$$

Now inserting (21) into (20) and simplifying with (22) and (23), we obtain the recursion

$$\|E_{n+1}\| \leq (1 + hL_*) \|E_n\| + h(\beta_1 + \beta_2),$$

where $L_* = \ell + \varphi_1(h\ell)L_{\mathcal{G}} + O(h)$, and the hidden constant in $O(h)$ depends only on ℓ and $L_{\mathcal{G}}$ (multiplied by φ -functions). Solving the recursion leads to

$$\|E_n\| \leq (1 + hL_*)^n \|E_0\| + h \sum_{k=0}^{n-1} (1 + hL_*)^k (\beta_1 + \beta_2), \quad (24)$$

Since we start from the initial value $X_0 = X(0)$, it holds $\|E_0\| = 0$. With the inequality

$$h \sum_{k=0}^{n-1} (1 + hL_*)^k \leq \frac{e^{nhL_*} - 1}{L_*},$$

we conclude that

$$\|X_n^R - X(t_n)\| \leq \frac{e^{nhL_*} - 1}{L_*} \cdot (\beta_1 + \beta_2).$$

For all $h \leq h_0$, the factor above reduces to a constant $C(\ell, L_{\mathcal{G}}, h_0)$ as stated in the theorem. \square

Remark 2. The exponential Runge methods (18) require the functions φ_1 and φ_2 . It is tempting to consider the following family of methods that only requires φ_1 :

$$\begin{array}{c|c} 0 & \\ \hline c_2 & c_2 \varphi_{1,2} \\ \hline & \left(1 - \frac{1}{2c_2}\right) \varphi_1 \quad \frac{1}{2c_2} \varphi_1 \end{array}$$

These methods have a classical order of two but their stiff order is strictly smaller than 2; see [11] for more details. Nevertheless, since their evaluation per step is much cheaper than the exponential Runge methods, they might be useful in some practical applications. In the following, we will refer to these methods as non-strict exponential Runge methods.

2.2 Dynamical low-rank approximation

Let \mathcal{M}_r denote the set of $m \times n$ matrices of rank r . It is a smoothly embedded submanifold in $\mathbb{R}^{m \times n}$ and its Riemannian geometry can be used effectively in numerical algorithms; see [14] for an overview.

Suppose the solution of the full problem (1) admits a good low-rank approximation. In that case, one can apply the dynamical low-rank approximation (DLRA) and solve a reduced problem instead. The technique is extensively studied in [1]. The corresponding DLRA of rank r is

$$\dot{Y}(t) = \mathcal{P}_{Y(t)} [\mathcal{L}Y(t) + \mathcal{G}(Y(t))], \quad Y(0) = Y_0 \in \mathcal{M}_r,$$

where \mathcal{P}_Y is the l_2 -orthogonal projection onto the tangent space $\mathcal{T}_Y \mathcal{M}_r$ of \mathcal{M}_r at $Y \in \mathcal{M}_r$,

$$\mathcal{P}_Y(Z) = UU^T Z + ZVV^T - UU^T ZVV^T \quad \text{with } Y = U\Sigma V^T \text{ a compact SVD,}$$

and $Y_0 \approx X_0$ is a (near) best rank approximation of X_0 . Since $\mathcal{L}Y \in \mathcal{T}_Y \mathcal{M}_r$, the equation simplifies to

$$\dot{Y}(t) = \mathcal{L}Y(t) + \mathcal{P}_{Y(t)} [\mathcal{G}(Y(t))], \quad Y(0) = Y_0. \quad (25)$$

Remark 3. *As long as the solution of (25) exists, it belongs to the manifold \mathcal{M}_r .*

Recall that $\phi_{\mathcal{F}}^t(X_0)$ denotes the flow of the full problem (1) at time t with initial value X_0 . Similarly, we denote by $\phi_{\mathcal{P}\mathcal{F}}^t(Y_0)$ the flow of the projected problem (25) with initial value $Y_0 \in \mathcal{M}_r$. The following assumption is standard when studying the approximation error made by DLRA.

Assumption 1 (DLRA assumption). *The function \mathcal{G} maps almost to the tangent bundle of \mathcal{M}_r :*

$$\|\mathcal{G}(Y) - \mathcal{P}_Y \mathcal{G}(Y)\| \leq \varepsilon_r,$$

for all Y in a neighborhood of the solution to the DLRA.

In terms of the total vector field, $\mathcal{F} = \mathcal{L} + \mathcal{G}$, the assumption above is equivalent to $\|\mathcal{F}(Y) - \mathcal{P}_Y \mathcal{F}(Y)\| \leq \varepsilon_r$ since \mathcal{L} maps to the tangent space. Using this property, we get immediately the following approximation result of DLRA (see [4] for a proof):

Theorem 7 (Accuracy of DLRA). *Assuming that $\mathcal{F} = \mathcal{L} + \mathcal{G}$ is one-sided Lipschitz with constant $\ell_{\mathcal{F}}$, and Assumption 1, the error made by the dynamical low-rank approximation of rank r verifies*

$$\|\phi_{\mathcal{F}}^t(X_0) - \phi_{\mathcal{P}\mathcal{F}}^t(Y_0)\| \leq e^{t\ell_{\mathcal{F}}} \|X_0 - Y_0\| + t\varphi_1(t\ell_{\mathcal{F}}) \varepsilon_r,$$

where \mathcal{F} represents the vector field of the full problem (1), and $\mathcal{P}\mathcal{F}$ that of the projected problem (25).

Recall the convenient bound $\ell_{\mathcal{F}} \leq \ell_{\mathcal{L}} + L_{\mathcal{G}}$ from Remark 1, showing that $\ell_{\mathcal{F}}$ can be negative for small non-linear perturbations \mathcal{G} with diffusive \mathcal{L} .

2.3 Contributions and outline

Even though they do not impose a particular structure to the problem, the projector-splitting algorithm [2] and the unconventional integrator [3] are not proven to be robust to stiff problems. In fact, Figure 1 shows that the two methods are numerically not robust to stiffness in general, even when a very small step size (10^{-5}) is used for the sub-steps. In addition, the projector-splitting algorithm contains a backward sub-step, making it not suitable for parabolic problems. More specialized methods are needed for stiff problems. Assuming the problem has a Sylvester-like structure, the low-rank splitting proposed in [6] is shown theoretically robust to stiffness but the method is not very useful in practice because of its large hidden constant. When the step size is $h \approx 0.01$, we can see in Figure 1 that its error is unreasonably large, though robust under mesh refinements. This paper's contribution is to fill the gap by proposing new methods of integration of DLRA for Sylvester-like structures that are robust to stiffness and have

small hidden error constants. As a motivation, Figure 1 shows that one of these new methods is accurate and robust under mesh refinements. More numerical experiments are detailed in Section 5.

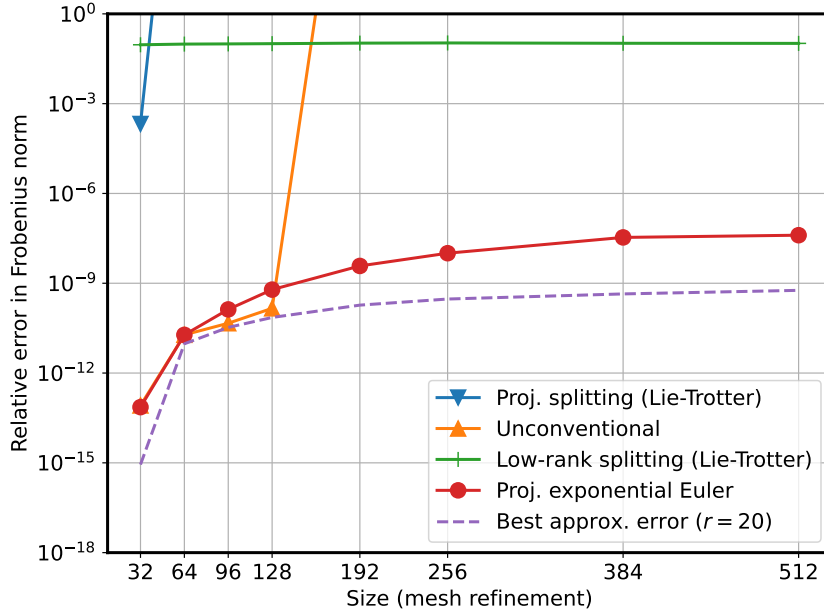


Fig. 1: Error of several methods under mesh refinements for solving the heat equation (stiff) that can be formulated as differential Lyapunov equation with constant source C ; see Section 5.1. Step size is $h = 0.01$.

The paper is organized as follows. Section 3 defines the new methods and derives theoretical guarantees. Section 4 describes an efficient implementation of the new methods, making this new method a practical integrator. Section 5 shows numerical experiments of the method and verifies the theoretical guarantees derived in the paper. Section 6 concludes and discusses potential future work directions.

3 Projected exponential methods

The definition of the (explicit) *projected exponential Runge-Kutta* (PERK) methods is naturally obtained from 6. We state them here for a method with s stages as

$$\begin{aligned}
 G_{nj} &= \mathcal{P}_{Y_{nj}} [\mathcal{G}(Y_{nj})], & \text{for } j = 1, \dots, s \\
 Y_{ni} &= \mathcal{T}_r \left(e^{c_i h \mathcal{L}} Y_n + h \sum_{j=1}^{i-1} a_{ij}(h\mathcal{L}) G_{nj} \right), & \text{for } i = 1, \dots, s \\
 Y_{n+1} &= \mathcal{T}_r \left(e^{h\mathcal{L}} Y_n + h \sum_{i=1}^s b_i(h\mathcal{L}) G_{ni} \right),
 \end{aligned} \tag{26}$$

where $\mathcal{T}_r: \mathbb{R}^{m \times n} \rightarrow \mathcal{M}_r$ represents taking a best rank r approximation of a matrix in Frobenius norm. Recall that this can be computed by truncating the SVD of the given matrix to its r dominant terms. We therefore call this operator the truncation operator. It is natural to consider using the same operators $a_{ij}(h\mathcal{L}), b_i(h\mathcal{L})$ and coefficients c_i as derived in the classical theory. Indeed, the projected methods coincide with the classical methods when $r = \min\{m, n\}$. Also, the same order conditions will appear in the expansion of the defects, as we will see later in the analysis.

The methods (26) are computationally attractive only when the internal stages remain of sufficiently low rank and when this is exploited in implementation. Thanks to the tangent space projection, $\text{rank}(G_{nj}) \leq 2r$ and the growth in rank comes mainly from the terms $\sum_{j=1}^s a_{ij}(h\mathcal{L}) G_{nj}$ and

$\sum_{i=1}^s b_i(h\mathcal{L})G_{ni}$. The computational and memory requirements will therefore grow with the number of internal stages s . However, compared to classical Runge–Kutta methods, the scaling is higher than linear in s due to the numerical linear algebra of low-rank calculations. We therefore limit our analysis to the one-stage and two-stage methods stated below.

3.1 Preliminary results

We start with Lemma 8 on the stability of the rank r truncation operator \mathcal{T}_r under perturbation. While it is well known that the Lipschitz constant of \mathcal{T}_r at $X \in \mathcal{M}_r$ behaves like $\sigma_r^{-1}(X)$, which would lead to undesirable bounds when $\sigma_r(X)$ is small, the operator \mathcal{T}_r is stable if we study the perturbation in an additive way. This result is similar to other results in the literature (see, e.g., [15, Lemma 4.1]) but we include the proof for completeness.

Lemma 8 (Truncation inequality). *Denote by \mathcal{T}_r the truncation to rank r . Then, for any two matrices A and E , we have*

$$\|\mathcal{T}_r(A + E) - A\| \leq \|\mathcal{T}_r(A) - A\| + 2\|E\|.$$

Proof. The triangular inequality gives

$$\|\mathcal{T}_r(A + E) - A\| = \|\mathcal{T}_r(A + E) - (A + E) + (A + E) - A\| \leq \|\mathcal{T}_r(A + E) - (A + E)\| + \|E\|,$$

and the conclusion follows from the definition of the best rank r approximation,

$$\begin{aligned} \|\mathcal{T}_r(A + E) - (A + E)\| &= \min_{\text{rank}(X) \leq r} \|X - (A + E)\| = \min_{\text{rank}(X) \leq r} \|X - A + A - (A + E)\| \\ &\leq \min_{\text{rank}(X) \leq r} \|X - A\|_F + \|E\| = \|\mathcal{T}_r(A) - A\| + \|E\|. \quad \square \end{aligned}$$

The factor two appearing in the truncation inequality above is inevitable and brings an extra challenge to the convergence proofs. Indeed, we cannot immediately express the numerical flow Y_n as a perturbation of the solution $X(t_n)$ nor $Y(t_n)$, since we would have a factor 2^n appearing when solving the recursion. The issue is bypassed by comparing instead the numerical flow with the DLRA started at the previous numerical solution $\phi_{P\mathcal{F}}^h(Y_n)$. This way, the exponential term is treated exactly and the undesirable factor 2^n does not appear. Similarly to the derivations made in Section 2.1, we derive a stable⁴ expansion of the projected field flow. The closed form formula (2) applied to the projected field (25) gives for $i = 1, \dots, s$

$$\phi_{P\mathcal{F}}^{c_i h}(Y_n) = e^{c_i h \mathcal{L}} Y_n + \int_0^{c_i h} e^{(c_i h - \tau) \mathcal{L}} \mathcal{P}_{\phi_{P\mathcal{F}}^\tau(Y_n)} [\mathcal{G}(\phi_{P\mathcal{F}}^\tau(Y_n))] d\tau. \quad (27)$$

The next step is to use $f(t) = \mathcal{G}(X(t))$ and decompose the projection as

$$\mathcal{P}_{\phi_{P\mathcal{F}}^\tau(Y_n)} [\mathcal{G}(\phi_{P\mathcal{F}}^\tau(Y_n))] = f(t_n + \tau) + \mathcal{P}_{\phi_{P\mathcal{F}}^\tau(Y_n)} [\mathcal{G}(\phi_{P\mathcal{F}}^\tau(Y_n))] - f(t_n + \tau).$$

Therefore, we obtain that

$$\phi_{P\mathcal{F}}^{c_i h}(Y_n) = e^{c_i h \mathcal{L}} Y_n + \int_0^{c_i h} e^{(c_i h - \tau) \mathcal{L}} f(t_n + \tau) d\tau + \Omega_{ni} + \Lambda_{ni},$$

where we have defined the two modelling defects

$$\Omega_{ni} = \int_0^{c_i h} e^{(c_i h - \tau) \mathcal{L}} [\mathcal{P}_{\phi_{P\mathcal{F}}^\tau(Y_n)} [\mathcal{G}(\phi_{P\mathcal{F}}^\tau(Y_n))] - \mathcal{G}(\phi_{P\mathcal{F}}^\tau(Y_n))] d\tau, \quad (28)$$

$$\Lambda_{ni} = \int_0^{c_i h} e^{(c_i h - \tau) \mathcal{L}} [\mathcal{G}(\phi_{P\mathcal{F}}^\tau(Y_n)) - f(t_n + \tau)] d\tau. \quad (29)$$

⁴Stable w.r.t. small singular values since the expansion does not involve derivatives of the projection.

By definition of Δ_{ni} in (12) we already have

$$\int_0^{c_i h} e^{(c_i h - \tau)\mathcal{L}} f(t_n + \tau) d\tau = \sum_{j=1}^{i-1} a_{ij}(h\mathcal{L}) f(t_n + c_j h) + \Delta_{ni},$$

and we therefore obtain the following expressions for the projected field flow:

$$\begin{aligned} \phi_{P\mathcal{F}}^{c_i h}(Y_n) &= e^{c_i h\mathcal{L}} Y_n + h \sum_{j=1}^{i-1} a_{ij}(h\mathcal{L}) f(t_n + c_j h) + \Delta_{ni} + \Omega_{ni} + \Lambda_{ni}, \\ \phi_{P\mathcal{F}}^h(Y_n) &= e^{h\mathcal{L}} Y_n + h \sum_{i=1}^s b_i(h\mathcal{L}) f(t_n + c_i h) + \delta_{n+1} + \omega_{n+1} + \lambda_{n+1}, \end{aligned} \quad (30)$$

where the second formula was derived in a similar manner. The next lemma bounds the modelling defects, and will be essential in the proof of convergence of the new methods.

Lemma 9 (Stable expansion of the projected flow). *Assume the function \mathcal{G} Lipschitz-continuous, and the function $f(t) = \mathcal{G}(X(t))$ sufficiently differentiable. Then, under Assumption 1 the projected field flow verifies the expansions (30) with terms Δ_{ni} and δ_{n+1} defined in (14), and modelling defects bounded by*

$$\begin{aligned} \|\Omega_{ni}\| &\leq c_i h \varphi_1(c_i h \ell) \varepsilon_r, \quad \|\omega_{n+1}\| \leq h \varphi_1(h \ell) \varepsilon_r, \\ \|\Lambda_{ni}\| &\leq L_{\mathcal{G}} \cdot c_i h \varphi_1(c_i h \ell) \cdot (1 + O(c_i h)) \cdot \|Y_n - X(t_n)\| + O((c_i h)^2) \cdot \varepsilon_r, \\ \|\lambda_{n+1}\| &\leq L_{\mathcal{G}} \cdot h \varphi_1(h \ell) \cdot (1 + O(h)) \cdot \|Y_n - X(t_n)\| + O(h^2) \cdot \varepsilon_r. \end{aligned}$$

Proof. Bounding the first modelling defect (28) requires Assumption 1, and a direct computation gives

$$\|\Omega_{ni}\| \leq \int_0^{c_i h} e^{(c_i h - \tau)\ell} \|\mathcal{P}_{\phi_{P\mathcal{F}}^\tau(Y_n)}[\mathcal{G}(\phi_{P\mathcal{F}}^\tau(Y_n))] - \mathcal{G}(\phi_{P\mathcal{F}}^\tau(Y_n))\| d\tau \leq c_i h \varphi_1(c_i h \ell) \varepsilon_r.$$

The statement for ω_{n+1} holds with a step size h instead of $c_i h$.

For the second modelling defect (29), we need to use the Lipschitz continuity of \mathcal{G} , and then Theorem 7 to get that

$$\begin{aligned} \|\Lambda_{ni}\| &\leq \int_0^{c_i h} e^{(c_i h - \tau)\ell} \cdot L_{\mathcal{G}} \cdot \|\phi_{P\mathcal{F}}^\tau(Y_n) - \phi_{\mathcal{F}}^\tau(X(t_n))\| d\tau \\ &\leq \int_0^{c_i h} e^{(c_i h - \tau)\ell} \cdot L_{\mathcal{G}} \cdot [e^{\tau\ell_{\mathcal{F}}} \|Y_n - X(t_n)\| + \tau \varphi_1(\tau \ell_{\mathcal{F}}) \varepsilon_r] d\tau. \end{aligned}$$

Computing the integrals and then simplifying with Taylor expansion gives

$$\begin{aligned} \int_0^{c_i h} e^{(c_i h - \tau)\ell} e^{\tau\ell_{\mathcal{F}}} d\tau &= \frac{e^{c_i h \ell} - e^{c_i h \ell_{\mathcal{F}}}}{\ell - \ell_{\mathcal{F}}} = c_i h \varphi_1(c_i h \ell) \cdot (1 + O(c_i h)), \\ \int_0^{c_i h} e^{(c_i h - \tau)\ell} \tau \varphi_1(\tau \ell_{\mathcal{F}}) d\tau &= \frac{\ell(1 - e^{c_i h \ell_{\mathcal{F}}}) + \ell_{\mathcal{F}}(e^{c_i h \ell} - 1)}{\ell \ell_{\mathcal{F}}(\ell - \ell_{\mathcal{F}})} = O((c_i h)^2). \end{aligned}$$

Since $\ell_{\mathcal{F}} \leq \ell + L_{\mathcal{G}}$, the hidden constants depend only on ℓ and $L_{\mathcal{G}}$ and they do not require a more explicit treatment in the analysis. \square

3.2 Projected exponential Euler

Similarly to the exponential Euler scheme (5), we define one step of the *projected exponential Euler* scheme:

$$Y_{n+1}^E = \mathcal{T}_r(e^{h\mathcal{L}} Y_n^E + h \varphi_1(h\mathcal{L}) \mathcal{P}_{Y_n^E}[\mathcal{G}(Y_n^E)]), \quad Y_n^E \in \mathcal{M}_r. \quad (31)$$

It corresponds to (26) where $b_1 = \varphi_1$ and $c_1 = 1$. The computational cost of (31) mainly comes from evaluating the φ -functions. In practice, these operators are never formed explicitly but their action on Y_n^E and $\mathcal{P}_{Y_n^E}[\mathcal{G}(Y_n^E)]$ is computed directly. In particular, since Y_n^E and $\mathcal{P}_{Y_n^E}[\mathcal{G}(Y_n^E)]$ have rank at most r and $2r$, resp., we can use Krylov techniques to approximate the action of these operators onto a tall matrix with at most $2r$ columns. A practical implementation that exploits even more structure will be detailed in Section 4. The following theorem states the convergence of the method.

Theorem 10 (Projected exponential Euler convergence). *Assume that \mathcal{G} is locally Lipschitz-continuous in a strip along the solution $X(t)$ to (1). Let Y_n^E be the n -th iteration of the projected exponential Euler scheme (31), and let $X(t_n)$ be the solution to (1) at time $t_n = nh$. Then, under Assumption 1 for $h \leq h_0$, the error verifies*

$$\|Y_n^E - X(t_n)\| \leq e^{t_n L_*} \cdot \|Y_0 - X_0\| + C_1 \cdot h \cdot \max_{0 \leq t \leq t_n} \left\| \frac{d}{dt} \mathcal{G}(X(t)) \right\| + C_2 \cdot \varepsilon_r,$$

where $L_* = \ell_{\mathcal{F}} + 4\varphi_1(h\ell)L_{\mathcal{G}} + O(h)$. The constants C_1 and C_2 are explicitly available in the proof and depend only on $\ell, L_{\mathcal{G}}, h_0$ and t_n but not on h, n nor the curvature of the manifold M_r .

Proof. We omit the notation \cdot^E in the proof. Let us define the error $E_{n+1} = Y_{n+1} - X(t_{n+1})$; we are going to find a recursion on the error as in the proof of Theorem 6 but with extra terms due to the modelling error induced by the DLRA. The factor two appearing in the retraction inequality from Lemma 8 forces us to treat exactly the exponential term $e^{h\mathcal{L}}Y_n$, so we need to work with the DLRA flow started at the numerical solution:

$$\|Y_{n+1} - X(t_{n+1})\| \leq \|\mathcal{T}_r(\phi_{\mathcal{P}\mathcal{F}}^h(Y_n) + K_{n+1}) - \phi_{\mathcal{P}\mathcal{F}}^h(Y_n) - M_{n+1}\| \leq 2\|K_{n+1}\| + \|M_{n+1}\|, \quad (32)$$

where we have defined

$$\begin{aligned} M_{n+1} &= \phi_{\mathcal{F}}^h(X(t_n)) - \phi_{\mathcal{P}\mathcal{F}}^h(Y_n), \\ K_{n+1} &= e^{h\mathcal{L}}Y_n + h\varphi_1(h\mathcal{L})\mathcal{P}_{Y_n}[\mathcal{G}(Y_n)] - \phi_{\mathcal{P}\mathcal{F}}^h(Y_n). \end{aligned}$$

The first difference term is easily bounded with Theorem 7:

$$\|M_{n+1}\| \leq e^{h\ell_{\mathcal{F}}} \|X(t_n) - Y_n\| + h\varphi_1(h\ell_{\mathcal{F}})\varepsilon_r. \quad (33)$$

The subtlety is in the second difference term K_{n+1} , for which we require the stable expansion of the projected flow derived in Section 3.1. Substituting $\phi_{\mathcal{P}\mathcal{F}}^h(Y_n)$ with (30) and applying Lemma 9 with $b_1 = \varphi_1$ gives that

$$\begin{aligned} \|K_{n+1}\| &\leq h\varphi_1(h\ell) \cdot \|\mathcal{P}_{Y_n}[\mathcal{G}(Y_n)] - f(t_n)\| + \|\delta_{n+1}\| + \|\omega_{n+1}\| + \|\lambda_{n+1}\| \\ &\leq h\varphi_1(h\ell) \cdot (2 + O(h)) \cdot L_{\mathcal{G}} \|E_n\| + h^2\varphi_2(h\ell) \cdot \max_{0 \leq s \leq h} \|f'(t_n + s)\| + 2h\varphi_1(h\ell)\varepsilon_r + O(h^2)\varepsilon_r. \end{aligned} \quad (34)$$

Inserting (34) and (33) into (32) gives the following recursion of the error $E_n^Y = Y_n - X(t_n)$:

$$\begin{aligned} \|E_{n+1}^Y\| &\leq (e^{h\ell_{\mathcal{F}}} + h\varphi_1(h\ell)L_{\mathcal{G}} \cdot (4 + O(h))) \|E_n^Y\| \\ &\quad + 2h^2\varphi_2(h\ell) \cdot \max_{0 \leq s \leq t_n} \|f'(s)\| + (4h\varphi_1(h\ell) + h\varphi_1(h\ell_{\mathcal{F}}))\varepsilon_r + O(h^2)\varepsilon_r \\ &\leq (1 + hL_*) \|E_n^Y\| + h(\beta + \gamma), \end{aligned}$$

where $L_* = \ell_{\mathcal{F}} + 4\varphi_1(h\ell)L_{\mathcal{G}} + O(h)$ and where we have defined

$$\beta = 2h\varphi_2(h\ell) \cdot \max_{0 \leq s \leq t_n} \|f'(s)\|, \quad \gamma = (4\varphi_1(h\ell) + \varphi_1(h\ell_{\mathcal{F}}) + O(h)) \cdot \varepsilon_r.$$

Finally, solving the recursion as we have already done in (24) leads to

$$\|E_n^Y\| \leq e^{nhL_*} \|Y_0 - X_0\| + \frac{e^{nhL_*} - 1}{L_*} \cdot (\beta + \gamma),$$

and by tracking the hidden constants, we see that they depend only on $\ell, L_{\mathcal{G}}$ and h_0 . \square

3.3 Projected exponential Runge

As we can see from Lemma 9, the remainder terms Δ_{ni} and δ_{n+1} are unchanged, and therefore the Butcher table 18 for the coefficients is still valid. The *projected exponential Runge* scheme iterates

$$\begin{aligned} Y_{n2}^R &= \mathcal{T}_r \left(e^{c_2 h \mathcal{L}} Y_n^R + c_2 h \varphi_1(c_2 h \mathcal{L}) \mathcal{P}_{Y_n^R} [\mathcal{G}(Y_n^R)] \right), \\ Y_{n+1}^R &= \mathcal{T}_r \left(e^{h \mathcal{L}} Y_n^R + h \varphi_1(h \mathcal{L}) \mathcal{P}_{Y_n^R} [\mathcal{G}(Y_n^R)] + h \varphi_2(h \mathcal{L}) \left(\mathcal{P}_{Y_{n2}^R} [\mathcal{G}(Y_{n2}^R)] - \mathcal{P}_{Y_n^R} [\mathcal{G}(Y_n^R)] \right) \right). \end{aligned} \quad (35)$$

This method has a good balance of numerical accuracy (order) and computational efficiency (cost per step). Even though the scheme (35) requires evaluating a φ_2 function, its computation is still manageable as we will show further in the implementation section. The main convergence theorem relies heavily on Lemma 9, but is similar in spirit to the proof of Theorem 6.

Theorem 11 (Projected exponential Runge convergence). *Assume \mathcal{G} sufficiently many times Fréchet differentiable in a strip along the exact solution and Assumption 1 satisfied. Let Y_n^R be the n -th step of the projected exponential Runge scheme started at $Y_0 \in \mathcal{M}_r$ with $c_2 > 0$, and $X(t_n)$ be the solution to the full problem (1). Then, under Assumption 1 for $h \leq h_0$, the error verifies*

$$\|Y_n^R - X(t_n)\| \leq e^{t_n L_*} \|Y_0 - X_0\| + C_1 \cdot h^2 \cdot \left(\max_{0 \leq t \leq t_n} \left\| \frac{d}{dt} \mathcal{G}(X(t)) \right\| + \max_{0 \leq t \leq t_n} \left\| \frac{d^2}{dt^2} \mathcal{G}(X(t)) \right\| \right) + C_2 \cdot \varepsilon_r,$$

where $L_* = \ell_F + 4\varphi_1(h\ell)L_G + O(h)$. The hidden constants depend only on ℓ, L_G, c_2, h_0 and t_n but not on h, n nor the curvature of the manifold \mathcal{M}_r .

Proof. Let us omit the notation \cdot^R . As in the proof of Theorem 10, we start by applying Lemma 8:

$$\|Y_{n+1} - X(t_{n+1})\| \leq \|\mathcal{T}_r(\phi_{\mathcal{P}\mathcal{F}}^h(Y_n) + K_{n+1}) - \phi_{\mathcal{P}\mathcal{F}}^h(Y_n) + M_{n+1}\| \leq 2\|K_{n+1}\| + \|M_{n+1}\|, \quad (36)$$

where, with the help of Lemma 9, we have

$$\begin{aligned} M_{n+1} &= \phi_{\mathcal{F}}^h(X(t_n)) - \phi_{\mathcal{P}\mathcal{F}}^h(Y_n), \\ K_{n+1} &= h \sum_{i=1}^2 b_i(h\mathcal{L}) [\mathcal{P}_{Y_{ni}} [\mathcal{G}(Y_{ni})] - f(t_n + c_i h)] - \delta_{n+1} - \omega_{n+1} - \lambda_{n+1}. \end{aligned}$$

The first difference term is, again, easily bounded by Theorem 7:

$$\|M_{n+1}\| \leq e^{h\ell_{\mathcal{F}}} \|X(t_n) - Y_n\| + h\varphi_1(h\ell_F) \cdot \varepsilon_r. \quad (37)$$

Bounding the second term involves the stage errors $E_{ni}^Y = Y_{ni} - X(t_n + c_i h)$ for $i = 1, 2$. From the definition of the stages, we immediately get that $\|E_{n1}^Y\| = \|Y_n - X(t_n)\|$ and

$$\|E_{n2}^Y\| = \|Y_{n2} - X(t_n + c_2 h)\| = \|\mathcal{T}_r(\phi_{\mathcal{P}\mathcal{F}}^{c_2 h}(Y_n) + K_{n2}) - \phi_{\mathcal{P}\mathcal{F}}^{c_2 h}(Y_n) + M_{n2}\| \leq 2\|K_{n2}\| + \|M_{n2}\|, \quad (38)$$

where K_{n2} and M_{n2} are difference terms. Here, we could use the expansion on the stages derived and bounded in Lemma 9. More concise is to notice that Y_{n2} coincides with exponential Euler with a step size of $c_2 h$, so its error bound is already derived in the course of the proof of Theorem 10:

$$\begin{aligned} \|E_{n2}^Y\| &\leq (e^{c_2 h \ell_{\mathcal{F}}} + c_2 h \varphi_1(c_2 h \ell) L_G \cdot (4 + O(c_2 h))) \|E_n^Y\| + (c_2 h)^2 \varphi_2(c_2 h \ell) \cdot \max_{0 \leq s \leq c_2 h} \|f'(t_n + s)\| + C \cdot h \cdot \varepsilon_r \\ &\leq (1 + c_2 h \tilde{L}) \|E_n^Y\| + (c_2 h)^2 \varphi_2(c_2 h \ell) \cdot \max_{0 \leq s \leq c_2 h} \|f'(t_n + s)\| + C \cdot h \cdot \varepsilon_r, \end{aligned} \quad (39)$$

where $\tilde{L} = \ell_{\mathcal{F}} + 4\varphi_1(c_2 h \ell) L_G + O(c_2 h)$. By the triangular inequality, we have that

$$\|K_{n+1}\| \leq h \sum_{i=1}^2 \|b_i(h\mathcal{L})\| \cdot (L_G \|Y_{ni} - X(t_n + c_i h)\| + \varepsilon_r) + \|\delta_{n+1}\| + \|\omega_{n+1}\| + \|\lambda_{n+1}\|, \quad (40)$$

where we have the following bounds:

$$\begin{aligned} \|\delta_{n+1}\| &\leq \tilde{C}_2 \cdot h^3 \cdot \max_{0 \leq s \leq h} \|f''(t_n + s)\|, & \|\omega_{n+1}\| &\leq h\varphi_1(h\ell)\varepsilon_r, \\ \text{and } \|\lambda_{n+1}\| &\leq L_G \cdot h\varphi_1(h\ell) \cdot (1 + O(h)) \cdot \|E_n\| + O(h^2) \cdot \varepsilon_r. \end{aligned} \quad (41)$$

The end of the proof consists essentially in assembling the terms together. Recall the bounds for b_1, b_2 from (23) and plugging (39) into (40) gives, after simplification, the following bound:

$$\|K_{n+1}\| \leq h \cdot L_G \cdot (2\varphi_1(h\ell) + O(h)) \|E_n^Y\| + \tilde{C}_1 \cdot h^3 \left(\max_{0 \leq s \leq h} \|f'(t_n + s)\| + \max_{0 \leq s \leq h} \|f''(t_n + s)\| \right) + \tilde{C}_2 \cdot h\varepsilon_r. \quad (42)$$

Now inserting (42) and (37) into (36) gives the following recursion for the error,

$$\|Y_{n+1} - X(t_{n+1})\| \leq (1 + hL_*) \|Y_n - X(t_n)\| + h(\beta + \gamma),$$

where we have defined the quantities $L_* = \ell_{\mathcal{F}} + 4\varphi_1(h\ell)L_G + O(h)$, and

$$\beta = \hat{C}_1 \cdot h^2 \cdot \left(\max_{0 \leq s \leq t_{n+1}} \|f'(s)\| + \max_{0 \leq s \leq t_{n+1}} \|f''(s)\| \right), \quad \gamma = \hat{C}_2 \cdot \varepsilon_r.$$

The conclusion follows since solving the recursion leads to

$$\|Y_n - X(t_n)\| \leq e^{nhL_*} \|Y_0 - X_0\| + \frac{e^{nhL_*} - 1}{L_*} (\beta + \gamma),$$

and keeping track of the hidden constants shows that they only depend on ℓ, L_G, c_2 and h_0 . \square

4 Efficient implementation with Krylov subspace techniques

Having proved the global error of the projected exponential Euler and Runge schemes, we will now explain their efficient implementation. As usual, the presence of the φ -functions requires special attention for large-scale problems. An added complication in our setting is that all computations should be done with low-rank approximations in mind. For example, storing or computing full matrices has to be avoided. Most of this section is therefore devoted in explaining how Krylov subspace approximation techniques for φ -functions can be performed efficiently with low-rank matrix approximations.

The efficient computation of $\varphi_k(hM)x$ given a vector x and a matrix M by Krylov subspace techniques is a well-studied topic. In case of the matrix exponential φ_0 , the earliest results go back to [16, 17]. The approximation of general φ -functions by Krylov spaces is a more recent topic discussed in [18] and by rational Krylov spaces in [9, 19]. Adaptive techniques are also described in [20, 21]. Good software implementations are also available. For standard Krylov subspaces, Expokit [22] allows computing the action of the matrix exponential. It is originally written in FORTRAN and MATLAB, and has been embedded into other languages, including Python. For rational Krylov methods, there exists the RKToolbox [23–27], which is written in MATLAB. Finally, when the matrix M is relatively small, dense linear algebra techniques for the matrix exponential are preferable and we refer to [28] for an efficient implementation in the context of φ -functions.

The techniques mentioned above can be used directly to implement the projected exponential methods proposed in this paper. However, a good implementation should exploit that the φ -functions are evaluated for $\mathcal{L} = I \otimes A + B^T \otimes I$, which has an important Kronecker structure. This is crucial when we want to obtain efficient low-rank approximations. The main idea is to build two independent Krylov subspaces for the range and co-range of the low-rank approximation. This is similar to Krylov methods that compute a low-rank approximation for *algebraic* Lyapunov and Sylvester equations; see, e.g., [29] for extended Krylov subspaces and [30] for a recent overview. Applied to differential Sylvester equations (hence, the ODE (1) with a constant function \mathcal{G}), such standard Krylov subspaces were already used in [31]. In [32], this was generalized to differential Riccati equations (hence, with $\mathcal{G}(X) = Q - X(t)SX(t)$) and analyzed for standard Krylov subspaces. The techniques proposed here find similarities with these methods, but

our approach treats the differential equation (1) with general \mathcal{G} and high-order exponential integrators. In addition, we analyze the error for rational Krylov subspaces.

4.1 Rational Krylov approximation

Before going into the details of the new technique, let us introduce basic notions of Krylov spaces. Given a generic (sparse) matrix $S \in \mathbb{R}^{m \times n}$ and a (tall) matrix $X \in \mathbb{R}^{n \times r}$, we define three variants of (block) Krylov spaces:

$$\begin{aligned} \text{Polynomial Krylov space: } & \mathcal{K}_k(S, X) = \text{span}\{X, SX, S^2X, \dots, S^{k-1}X\}, \\ \text{Extended Krylov space: } & EK_k(S, X) = \mathcal{K}_k(S, X) + \mathcal{K}_k(S^{-1}, S^{-1}X), \\ \text{Rational Krylov space: } & RK_k(S, X) = q_{k-1}(S)^{-1}\mathcal{K}_k(S, X), \quad \text{for a degree } k-1 \text{ polynomial } q_{k-1}. \end{aligned}$$

An extended Krylov space requires that S is invertible. For the construction of the rational Krylov space, one typically uses the factored polynomial $q_{k-1}(z) = (z - \rho_1) \cdots (z - \rho_{k-1})$. To ensure the invertibility of $q_{k-1}(S)$, the poles $\rho_1, \dots, \rho_{k-1}$ have to be different from the eigenvalues of S . Observe that the poles are part of the definition of $RK_k(S, X)$ and can be fixed from the start or adaptively during the iteration. We will focus on the former for simplicity.

Computing orthonormal bases for these block Krylov spaces requires some care but can be done efficiently with the (rational) Arnoldi algorithm; we refer to [33] for a MATLAB implementation. Good (and even optimal) choices of the poles are discussed in [34].

In the following, a generic Krylov space $GK_k(s, X)$ will refer to any of these spaces. The matrix S represents a generic matrix (operator) but will always be A or B from (1) in the following. Polynomial Krylov spaces are the least expensive to compute per step but they also have the worst approximation error leading to many iterations and thus higher memory requirements. Rational Krylov spaces have the best approximation error but they require determining the poles and their application per step is expensive. On the other hand, they typically require less iterations and, therefore, have a low memory footprint. Extended Krylov spaces are the compromise between these two techniques if linear systems with S are feasible to compute.

While any of these methods can be used, we will focus our analysis on rational Krylov spaces since they are the most memory efficient. The following lemma will be useful later in the analysis. It relates the rational Krylov approximation of $e^{tS}X$ to that of the best rational approximant of e^t . The latter has a long history and many results are known depending on the way the poles are determined; see the references in [34]. We have chosen to give one of the more elegant results when S is a symmetric matrix with strictly negative eigenvalue, hence $\ell_S < 0$. In the context of stiffness, this situation is actually very relevant. One can allow non-symmetric matrices as well using the field of values, but we do not give details for simplicity.

Lemma 12 (Error made by rational Krylov approximation on the exponential function). *Consider a symmetric matrix $S \in \mathbb{R}^{n \times n}$ with $\ell_S = \lambda_{\max}(S) < 0$ and a matrix $X \in \mathbb{R}^{n \times m}$. Let Q_k be such that $Q_k^T Q_k = I$ and $\text{span}(Q_k) = RK_k(S, X)$ with $RK_k(S, X)$ the rational Krylov space with optimal poles $\rho_1, \dots, \rho_{k-1}$ as defined in the proof. Denote $S_k = Q_k^T S Q_k$. Then, for all $t \geq 0$ it holds*

$$\|e^{tS}X - Q_k e^{tS_k} Q_k^T X\| \leq \frac{2\sqrt{2}}{3^{k-1}} \|X\|.$$

In the asymptotic regime $k \rightarrow \infty$, the constant 3 can be improved to at least 9.037.

Proof. Let Π_{k-1} be the set of polynomials of degree at most $k-1$. By Lemma 3.2 in [35], the block rational Krylov approximation has the exactness property

$$r(S)X = Q_k r(Q_k^T S Q_k) Q_k^T X \quad \forall r = p/q_{k-1}, p \in \Pi_{k-1}.$$

Here, $q_{k-1} \in \Pi_{k-1}$ depends on the poles that we leave undetermined for now. From this and the fact that $RK_k(S, X) = RK_k(tS, X)$ for nonzero t , we obtain that the rational Krylov approximation error of

the exponential is never worse than that by any rational function r as defined above,

$$\begin{aligned} \|e^{tS}X - Q_k e^{tS_k} Q_k^T X\| &= \|e^{tS}X - r(tS)X + Q_k r(tQ_k^T S Q_k) Q_k^T X - Q_k e^{tS_k} Q_k^T X\| \\ &\leq (\|e^{tS} - r(tS)\|_2 + \|e^{tS_k} - r(tQ_k^T S Q_k)\|_2) \|X\|. \end{aligned}$$

Since S and $Q_k^T S Q_k$ are symmetric, the approximation errors above can be calculated on their spectrum. Both matrices having negative eigenvalues and $t \geq 0$, we can therefore bound

$$\|e^{tS}X - Q_k e^{tS_k} Q_k^T X\| \leq 2 \|X\| \sup_{z \in [0, \infty)} |e^{-z} - r(-z)|. \quad (43)$$

Recall that $r = p/q_{k-1}$ such that $p \in \Pi_{k-1}$ was arbitrary and $q_{k-1} \in \Pi_{k-1}$ depends on the still to be fixed poles. Hence, we can take the infimum of (43) over all such rational functions r . By classical results in approximation theory (see, e.g., [36, Thm. 4.11]), we have

$$\inf_r \sup_{z \in [0, \infty)} |e^{-z} - r(-z)| = \frac{\sqrt{2}}{3^{k-1}}.$$

Combining leads to the desired result with the poles taken from the best approximant r_* above. The statement about the asymptotic improvement is also in [36, Chap. 4.5] and [37]. \square

4.2 Lucky Krylov approximation

In this section, we explain how to exploit the structure of the projected exponential methods (26) and perform efficient computations. In [1, Lemma 4.1], it is shown that the projection satisfies

$$\mathcal{P}_Y [\mathcal{G}(Y)] = UU^T \mathcal{G}(Y) - UU^T \mathcal{G}(Y) VV^T + \mathcal{G}(Y) VV^T, \quad (44)$$

where $Y = U\Sigma V^T$ is a compact SVD decomposition. The key idea in our implementation is to exploit that Y can be represented in the same subspace that is used for $\mathcal{P}_Y [\mathcal{G}(Y)]$, independent of \mathcal{G} . Together with Lemma 2, we will show that the sub-steps of the projected exponential methods can then be computed all-at-once in an efficient manner with Krylov techniques.

First order: projected exponential Euler

Recall the projected exponential Euler scheme (31):

$$Y_1 = \mathcal{T}_r (\tilde{Y}_1) = \mathcal{T}_r (e^{h\mathcal{L}} Y_0 + h\varphi_1(h\mathcal{L}) \mathcal{P}_{Y_0} [\mathcal{G}(Y_0)]). \quad (45)$$

The naive approach would be to compute its vectorized formulation,

$$\text{vec}(\tilde{Y}_1) = e^{h\mathcal{L}} \text{vec}(Y_0) + h\varphi_1(h\mathcal{L}) \text{vec}(\mathcal{P}_{Y_0} [\mathcal{G}(Y_0)]),$$

using classical Krylov techniques for exponential functions, as described in [22] and [28]. However, one would have to form dense matrices, which makes such an approach very inefficient. Fortunately, it is possible to reduce the computational cost by smartly exploiting the Sylvester-like structure.

By Lemma 2, the term inside the truncation can be obtained as $Z(h)$ where Z satisfies the following Sylvester differential equation:

$$Z(t) = e^{t\mathcal{L}} Y_0 + t\varphi_1(t\mathcal{L}) \mathcal{P}_{Y_0} [\mathcal{G}(Y_0)] \iff \begin{cases} \dot{Z}(t) = AZ(t) + Z(t)B + \mathcal{P}_{Y_0} [\mathcal{G}(Y_0)], \\ Z(0) = Y_0. \end{cases} \quad (46)$$

Since $Y_0 \in \mathcal{M}_r$ and $\mathcal{P}_{Y_0} [\mathcal{G}(Y_0)] \in \mathcal{T}_{Y_0} \mathcal{M}_r$, these matrices can be represented using the SVD as

$$Y_0 = U_0 \Sigma V_0^T \quad \text{where } \Sigma \in \mathbb{R}^{r \times r}, U_0 \in \mathbb{R}^{n \times r}, V_0 \in \mathbb{R}^{m \times r};$$

$$\mathcal{P}_{Y_0} [G(Y_0)] = [U_0, U_1] \tilde{\Sigma} [V_0, V_1]^T \quad \text{where } \tilde{\Sigma} \in \mathbb{R}^{2r \times 2r}, U_1 \in \mathbb{R}^{n \times r}, V_1 \in \mathbb{R}^{m \times r}.$$

Observe that Y_0 can be represented in the bases for the range and co-range of $\mathcal{P}_{Y_0} [G(Y_0)]$. It is therefore natural to consider the following two Krylov spaces

$$\begin{aligned} Q_k &\text{ is a matrix with orthonormal columns s.t. } \quad \text{span}(Q_k) = GK_k(A, \text{span}([U_0, U_1])), \\ W_k &\text{ is a matrix with orthonormal columns s.t. } \quad \text{span}(W_k) = GK_k(B, \text{span}([V_0, V_1])), \end{aligned}$$

Then, we perform a Galerkin projection to obtain a reduced Sylvester differential equation,

$$\begin{cases} \dot{S}_k(t) = Q_k^T A Q_k S_k(t) + S_k(t) W_k^T B W_k + Q_k^T \mathcal{P}_{Y_0} [G(Y_0)] W_k \\ S_k(0) = Q_k^T Y_0 W_k \end{cases} \quad (47)$$

where $S_k(t) \in \mathbb{R}^{2kr \times 2kr}$. Let us denote $A_k = Q_k^T A Q_k$ and $B_k = W_k^T B W_k$. When the Sylvester operator is invertible, the closed-form solution is given by (see, e.g., [31])

$$S_k(t) = e^{tA_k} (S_k(0) + C) e^{tB_k} - C, \quad A_k C + C B_k = Q_k^T \mathcal{P}_{Y_0} [G(Y_0)] W_k,$$

where the second equation is an algebraic Sylvester equation. These computations are feasible since the dimension is much smaller than in (46). In particular, it can be evaluated in $O(k^3 r^3)$ flops with techniques from dense linear algebra for computing the matrix exponential [38] and solving the algebraic Sylvester equation [39]. Alternatively, any integrator for stiff ODEs can be used for computing the solution to the reduced IVP. Finally, with the approximated solution $S_k(h)$ of (46) we can define

$$\tilde{Y}_1 = Z(h) \approx Z_k(h) = Q_k S_k(h) W_k^T. \quad (48)$$

Second order: projected exponential Runge

Let us recall the second-order scheme (35) with $c_2 = 1$:

$$\begin{aligned} Y_{1/2}^{\text{PR}} &= \mathcal{T}_r \left(e^{h\mathcal{L}} Y_0 + h\varphi_1(h\mathcal{L}) \mathcal{P}_{Y_0} [G(Y_0)] \right), \\ Y_1^{\text{PR}} &= \mathcal{T}_r \left(e^{h\mathcal{L}} Y_0 + h\varphi_1(h\mathcal{L}) \mathcal{P}_{Y_0} [G(Y_0)] + h\varphi_2(h\mathcal{L}) \left(\mathcal{P}_{Y_{1/2}^{\text{PR}}} [G(Y_{1/2}^{\text{PR}})] - \mathcal{P}_{Y_0} [G(Y_0)] \right) \right). \end{aligned}$$

The term $Y_{1/2}^{\text{PR}}$ can be approximated with the first order approximation described above. Similarly, we use Lemma 2 for treating the term Y_1^{PR} . The term inside the truncation is equivalent to $Z(h)$ where Z satisfies the initial value problem

$$\begin{cases} \dot{Z}(t) = AZ(t) + Z(t)B + \mathcal{P}_{Y_0} [G(Y_0)] + \frac{t}{h} \left[\mathcal{P}_{Y_{1/2}^{\text{PR}}} [G(Y_{1/2}^{\text{PR}})] - \mathcal{P}_{Y_0} [G(Y_0)] \right], \\ Z(0) = Y_0. \end{cases} \quad (49)$$

By the SVD, we can write

$$Y_0 = U_0 \Sigma V_0^T, \quad \mathcal{P}_{Y_0} [G(Y_0)] = [U_0, U_1] \tilde{\Sigma} [V_0, V_1]^T, \quad \mathcal{P}_{Y_{1/2}^{\text{PR}}} [G(Y_{1/2}^{\text{PR}})] = U_2 \hat{\Sigma} V_2^T,$$

for some matrices $\Sigma \in \mathbb{R}^{r \times r}$, $\tilde{\Sigma} \in \mathbb{R}^{2r \times 2r}$, and $\hat{\Sigma} \in \mathbb{R}^{2r \times 2r}$. Clearly all three matrices can be represented in the subspaces $[U_0, U_1, U_2]$ and $[V_0, V_1, U_2]$, each of dimension $4k$. While in general $\text{span}(U_2) \not\subset \text{span}([U_0, U_1])$, these subspaces are close for small step size h . It is therefore reasonable to truncate these approximation subspaces to lower dimension in practice. In any case the structure suggests using two Krylov spaces such that

$$\begin{aligned} Q_k &\text{ is a matrix with orthonormal columns s.t. } \quad \text{span}(Q_k) = GK_k(A, \text{span}([U_0, U_1, U_2])), \\ W_k &\text{ is a matrix with orthonormal columns s.t. } \quad \text{span}(W_k) = GK_k(B, \text{span}([V_0, V_1, U_2])). \end{aligned}$$

The reduced system is then obtained by a Galerkin projection,

$$\begin{cases} \dot{S}_k(t) = A_k S_k(t) + S_k(t) B_k + Q_k^T \mathcal{P}_{Y_0} [\mathcal{G}(Y_0)] W_k + \frac{t}{h} Q_k^T \left[\mathcal{P}_{Y_{1/2}^{\text{PR}}} [\mathcal{G}(Y_{1/2}^{\text{PR}})] - \mathcal{P}_{Y_0} [\mathcal{G}(Y_0)] \right] W_k, \\ S_k(0) = Q_k^T Y_0 W_k, \end{cases} \quad (50)$$

where $A_k = Q_k^T A Q_k$, $B_k = W_k^T B W_k$, and $S_k(t) \in \mathbb{R}^{4kr \times 4kr}$. Again, when the Sylvester operator is invertible, the closed form solution is given by

$$\begin{aligned} h \cdot (A_k \hat{D} + \hat{D} B_k) &= D, \quad A_k D + D B_k = Q_k^T \left[\mathcal{P}_{Y_{1/2}^{\text{PR}}} [\mathcal{G}(Y_{1/2}^{\text{PR}})] - \mathcal{P}_{Y_0} [\mathcal{G}(Y_0)] \right] W_k, \\ A_k C + C B_k &= Q_k^T \mathcal{P}_{Y_0} [\mathcal{G}(Y_0)] W_k, \\ S_k(t) &= e^{t A_k} \left(S_k(0) + C + \hat{D} \right) e^{t B_k} - C - \hat{D} - D, \end{aligned}$$

where the matrices C , D , and \hat{D} are obtained by solving algebraic Sylvester equations at a cost of $O(k^3 r^3)$ flops. Alternatively, the reduced system (50) can be solved by any numerical integrator for stiff ODEs. The final approximation is

$$\tilde{Y}_1^{\text{PR}} = Z(h) \approx Z_k(h) = Q_k S_k(h) W_k^T. \quad (51)$$

Remark 4. *The procedure immediately extends to any higher-order scheme with s stages. It requires computing $2s$ different Krylov spaces in total. The largest reduced system will have size $2skr$, at maximum leading to a cost of $O(s^3 k^3 r^3)$ flops. In practice, it is likely that the subspaces of the sub-steps are not strictly orthogonal leading to lower dimensional systems.*

4.3 A priori approximation bounds

The following results give a priori convergence bounds for the approximation error when rational Krylov spaces are used. These bounds can be used for estimating the size of the Krylov spaces (that is, the number of iterations in the Arnoldi iteration). A similar bound is derived in [32] for polynomial Krylov spaces. Our results extend it to rational Krylov spaces and to higher-order schemes.

Theorem 13 (Rational Krylov approximation error, Euler scheme). *Let $Z(t)$ be the solution to the full differential Sylvester equation (46) with symmetric and negative definite matrices A and B . Let $Z_k(t) = Q_k S_k(t) W_k^T$ with $S_k(t)$ be the solution to the reduced differential Sylvester equation (47) obtained with a rational Krylov space with $k - 1$ poles as in Lemma 12. Then, the error of the approximation (48) satisfies*

$$\|Z(h) - Z_k(h)\| \leq \frac{4\sqrt{2}}{3^{k-1}} \left(e^{h\ell_*} \|Y_0\| + \frac{e^{h\ell_*} - 1}{\ell_*} \|\mathcal{P}_{Y_0} \mathcal{G}(Y_0)\| \right)$$

where $\ell_* = \max(\ell_A, \ell_B) \leq 0$. Asymptotically, the constant 3 improves to at least 9.

Proof. The closed-form solutions satisfy

$$\begin{aligned} Z(t) &= e^{tA} Y_0 e^{tB} + \int_0^t e^{(t-s)A} \mathcal{P}_{Y_0} [\mathcal{G}(Y_0)] e^{(t-s)B} ds, \\ Z_k(t) &= Q_k e^{tA_k} Q_k^T Y_0 W_k e^{tB_k} W_k^T + \int_0^t Q_k e^{(t-s)A_k} Q_k^T \mathcal{P}_{Y_0} [\mathcal{G}(Y_0)] W_k e^{(t-s)B_k} W_k^T ds, \end{aligned}$$

where $A_k = Q_k^T A Q_k$ and $B_k = W_k^T B W_k$. Let us decompose the error as

$$Z(t) - Z_k(t) = E_k^1(t) + E_k^2(t),$$

where

$$E_k^1(t) = e^{tA} Y_0 e^{tB} - Q_k e^{tA_k} Q_k^T Y_0 W_k e^{tB_k} W_k^T,$$

$$E_k^2(t) = \int_0^t e^{(t-s)A} \mathcal{P}_{Y_0} [\mathcal{G}(Y_0)] e^{(t-s)B} - Q_k e^{(t-s)A_k} Q_k^T \mathcal{P}_{Y_0} [\mathcal{G}(Y_0)] W_k e^{(t-s)B_k} W_k^T ds.$$

Applying Lemma 12 twice, the norm of the first term is bounded as

$$\begin{aligned} \|E_k^1(t)\| &= \|e^{tA} Y_0 e^{tB} - Q_k e^{tA_k} Q_k^T Y_0 e^{tB} + Q_k e^{tA_k} Q_k^T Y_0 e^{tB} - Q_k e^{tA_k} Q_k^T Y_0 W_k e^{tB_k} W_k^T\| \\ &= \|(e^{tA} - Q_k e^{tA_k} Q_k^T) Y_0 e^{tB}\| + \|Q_k e^{tA_k} Q_k^T Y_0 (e^{tB} - W_k e^{tB_k} W_k^T)\| \\ &\leq \frac{2\sqrt{2}}{3^{k-1}} \cdot \|Y_0\| \cdot (\|e^{tB}\| + \|Q_k e^{tA_k} Q_k^T\|). \end{aligned}$$

With Lemma 3 and $\ell_* = \max(\ell_A, \ell_B)$ we obtain

$$\|E_k^1(t)\| \leq \frac{4\sqrt{2}}{3^{k-1}} \cdot e^{t\ell_*} \|Y_0\|.$$

By a similar argument, the norm of the second term is bounded as follows

$$\begin{aligned} \|E_k^2(t)\| &\leq \int_0^t \frac{2\sqrt{2}}{3^{k-1}} \cdot \|\mathcal{P}_{Y_0} [\mathcal{G}(Y_0)]\| \cdot (\|e^{(t-s)B}\| + \|Q_k e^{(t-s)A_k} Q_k^T\|) ds \\ &\leq \frac{4\sqrt{2}}{3^{k-1}} \cdot \|\mathcal{P}_{Y_0} [\mathcal{G}(Y_0)]\| \cdot \int_0^t e^{(t-s)\ell_*} ds \\ &= \frac{4\sqrt{2}}{3^{k-1}} \cdot \frac{e^{t\ell_*} - 1}{\ell_*} \|\mathcal{P}_{Y_0} [\mathcal{G}(Y_0)]\|. \end{aligned}$$

Substituting $t = h$ gives the desired result. \square

Thanks to the fast exponential convergence in k , this theorem implies that the intermediate matrix \tilde{Y}_1 in the projected exponential Euler method (45) can be accurately computed in practice with only a few steps of the rational Krylov method. Since the rank of \tilde{Y}_1 is bounded by $2kr$, its rank will also not grow much and the truncation operator in (45) can be applied efficiently. Furthermore, the approximation error does not depend on the Lipschitz constant of \mathcal{L} and is thus also robust to stiffness.

The following result shows that essentially the same properties remain to hold for the projected exponential Runge scheme.

Theorem 14 (Rational Krylov approximation error, Runge scheme). *Let $Z(t)$ be the solution to the full differential Sylvester equation (49) with symmetric and negative definite matrices A and B . Let $Z_k(t) = Q_k S_k(t) W_k^T$ with $S_k(t)$ be the solution to the reduced differential Sylvester equation (50) obtained with a rational Krylov space with $k - 1$ poles as in Lemma 12. Then, the error of the approximation (51) satisfies*

$$\|Z(h) - Z_k(h)\| \leq \frac{4\sqrt{2}}{3^{k-1}} \left(e^{h\ell_*} \|Y_0\| + \frac{e^{h\ell_*} - 1}{\ell_*} \|\mathcal{P}_{Y_0} \mathcal{G}(Y_0)\| + \frac{e^{h\ell_*} - 1 - h\ell_*}{h\ell_*^2} \|D\| \right),$$

where $\ell_* = \max(\ell_A, \ell_B) \leq 0$ and $D = \mathcal{P}_{Y_{1/2}^{\text{PR}}} [\mathcal{G}(Y_{1/2}^{\text{PR}})] - \mathcal{P}_{Y_0} [\mathcal{G}(Y_0)]$. Asymptotically, the constant 3 improves to at least 9.

Proof. Let us define the two terms $E_k^1(t)$ and $E_k^2(t)$ as in the proof of Theorem 13. Writing down the closed-form formula for the solution $Z(t)$, we get the additional term

$$E_k^3(t) = \frac{1}{h} \int_0^t s \left[e^{(t-s)A} D e^{(t-s)B} - Q_k e^{(t-s)A_k} Q_k^T D W_k e^{(t-s)B_k} W_k^T \right] ds.$$

Taking its norm, we bound it like the terms $E_k^1(t)$ and $E_k^2(t)$ as follows

$$\|E_k^3(t)\| \leq \frac{4\sqrt{2}}{3^{k-1}} \cdot \frac{1}{h} \int_0^t s e^{(t-s)\mu_*} \|D\| ds = \frac{4\sqrt{2}}{3^{k-1}} \frac{e^{t\mu_*} - 1 - t\mu_*}{h\mu_*^2} \|D\|. \quad \square$$

Remark 5. *The approximation bounds above extend easily to any linear combination of φ -functions and, therefore, to any higher-order (projected) exponential scheme.*

5 Numerical experiments

In this section, we test the proposed integrators numerically with stiff examples that contain a diffusion component. We start with the differential Lyapunov equation, where we show basic properties of the new methods. Then, we consider the Riccati differential equation, where we compare the new methods to existing methods. Moreover, we inspect the error made by the Krylov approximation techniques and compare them to the theoretical bounds derived in the previous section. Next, we demonstrate the capabilities of the new methods on the Allen-Cahn equation, when the non-linearity is not “tangent space friendly”. Finally, we propose a rank-adaptive variant of the methods and show its numerical behavior.

The implementation is done in Python and the experiments were performed on a MacBook Pro with M1 processor and 16GB of RAM, except for Figure 2 which required more memory and was performed on a workstation running Ubuntu 20.04 with an Intel i9-9900k processor and 64GB of RAM. All numerical experiments can be reproduced with the open source code available on [GitHub](#)⁵.

5.1 Application to the differential Lyapunov equation

We consider the Lyapunov differential equation

$$\dot{X}(t) = AX(t) + X(t)A^T + C(t), \quad X(0) = X_0, \quad (52)$$

where $A \in \mathbb{R}^{n \times n}$ is sparse, and $C(t) \in \mathbb{R}^{n \times n}$ is a symmetric low-rank matrix. The differential Lyapunov equation appears in discretized partial differential equations; but also in other areas, such as stability analysis, controller design for linear time-varying systems [40], and optimal control of linear time-invariant systems on finite time horizons [41], to name a few. To demonstrate basic properties, we consider the partial differential equation modelling heat propagation⁶ with Dirichlet boundary conditions,

$$\begin{cases} \partial_t u(\mathbf{x}, t) = \Delta u(\mathbf{x}, t) + s(\mathbf{x}, t), & \mathbf{x} \in \Omega, \quad t \in [0, T], \\ u(\mathbf{x}, 0) = \mathbf{u}_0, & \mathbf{x} \in \Omega, \\ u(\mathbf{x}, t) = 0, & \mathbf{x} \in \partial\Omega, \quad t \in [0, T]. \end{cases} \quad (53)$$

With two spatial dimensions, the discretized problem on a tensor grid (like standard finite differences) is exactly a Lyapunov differential equation where A is the one-dimensional finite-difference stencil, and $C(t)$ is the discretization of the source $s(\mathbf{x}, t)$. It is shown in [42] that, under a few conditions, the solution admits a good low-rank approximation.

In the following, the problem is solved on the time-interval $[0, T] = [0, 1]$ and the spatial domain is $\Omega = [0, 1]^2$. If not mentioned otherwise, the size of the problem is $n = 128$ (corresponding to $n^2 = 16384$ dofs), and the step size is $h = 0.001$. For this mesh refinement, the problem is moderately stiff. An implicit method should be preferred, but an explicit method can still be used if the time steps are sufficiently small. We use extended Krylov spaces with only one iteration, so $EK(A, X) = \text{span}\{X, A^{-1}X\}$.

The motivating example above, Figure 1, was produced with a constant source term defined by the symmetric low-rank matrix

$$C(t) = Q\Sigma Q^T \in \mathbb{R}^{n \times n}, \quad \text{diag}(\Sigma) = \{1, 10^{-4}, 10^{-8}, 10^{-12}, 10^{-16}\},$$

and $Q \in \mathbb{R}^{n \times 5}$ is a random matrix with orthonormal columns. In this figure, we observe that the projected exponential Euler method is close to the approximation error. In fact, the source is constant so its derivative is zero and, therefore, Theorem 10 predicts that the method is exact, up to the approximation error due to the rank and the Krylov space.

⁵The URL is: <https://github.com/BenjaminCarrel/projected-exponential-methods>

⁶The heat propagation is the archetypal example of a stiff problem.

In the next experiments, we introduce a source term as defined in [6], but time-dependent. We consider the q independent vectors $\{\mathbf{1}, \mathbf{e}_1, \dots, \mathbf{e}_{(q-1)/2}, \mathbf{f}_1, \dots, \mathbf{f}_{(q-1)/2}\}$, where

$$e_k(x) = \sqrt{2} \cos(2\pi kx) \quad \text{and} \quad f_k(x) = \sqrt{2} \sin(2\pi kx), \quad k = 1, \dots, (q-1)/2,$$

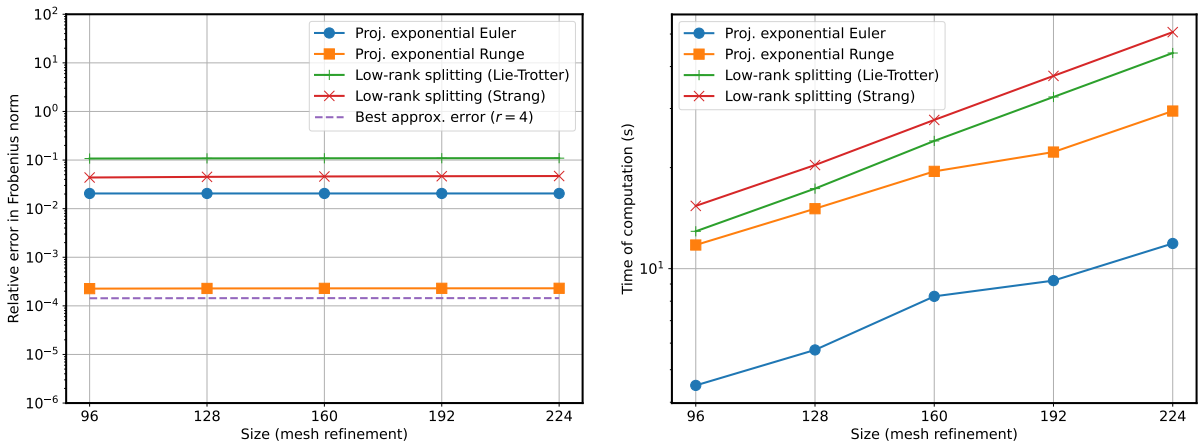
are evaluated at the grid points $\{x_j\}_{j=1}^n$ with $x_j = \frac{j}{n+1}$. Then, the time-dependent source is defined as

$$C(t) = e^{4t} \cdot M^T M, \quad M = \begin{bmatrix} \mathbf{1} & \mathbf{e}_1 & \dots & \mathbf{e}_{(q-1)/2} & \mathbf{f}_1 & \dots & \mathbf{f}_{(q-1)/2} \end{bmatrix}.$$

In the following, we take $q = 5$. The matrix M will also be used in the Riccati experiments but with $q = 9$.

Mesh refinements and performance

In Figure 2, we investigate the stability of the algorithms under mesh refinements. It is similar to the previous figure, but now with a time-dependent source and including second order methods. As we can see, our new methods are noticeably more accurate and also faster, in addition to being more precise than the existing techniques from [6] based on low-rank splittings. Despite the mesh refinements; the errors remain stable, which verifies the robust-to-stiffness property of the methods.



(a) Relative error at final time under mesh refinements. (b) Total time of computation for each mesh size.

Fig. 2: New methods applied to the differential Lyapunov equation with time-dependent source. The low-rank splitting techniques are from [6].

Rank and performance

Another important property for a low-rank method is to be robust to small singular values. In other words, the methods have to remain stable in the presence of small singular values, which is generally observed since we desire small error due to finite rank. In Figure 3, we applied projected exponential Runge (35) with several ranks of approximation. Clearly, the convergence properties do not depend on the choice of the rank, which only limits the accuracy due to the low-rank approximation. For this particular problem, the method shows very good performance, even when the rank increases.

Non strict order conditions

As mentioned in Remark 2, weakening the second order condition leads to a method that has classical order two but not stiff order two. In Figure 4, we compare the error of projected exponential Runge with strict order conditions and its non strict equivalent. While the non-strict method does not have robust order two in theory, it performs very well in practice. As we can see, the non-strict method has a slightly larger hidden constant than its strict equivalent, and the same convergence rate of two. It is, therefore,

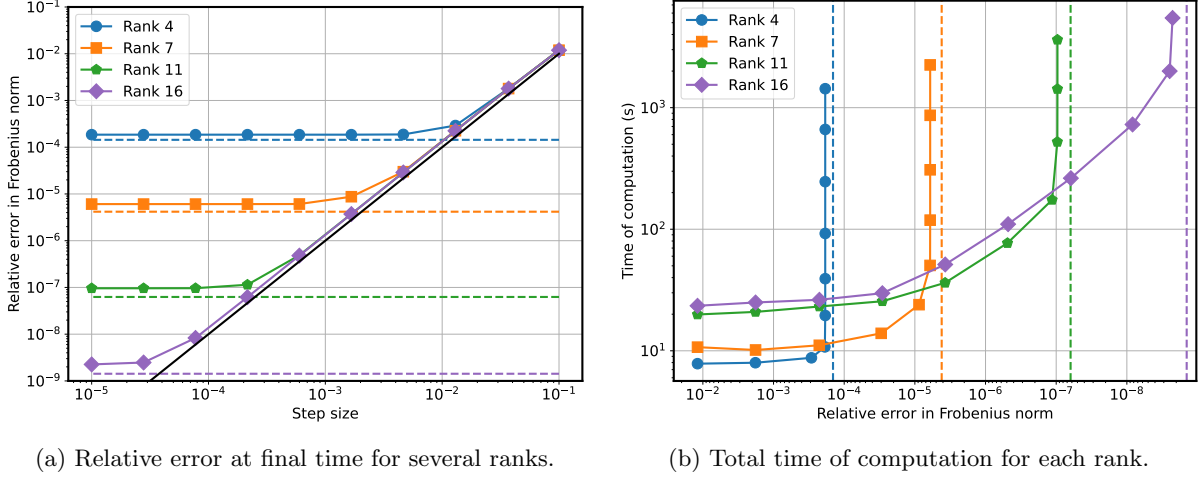


Fig. 3: Projected exponential Runge (35) applied to differential Lyapunov equation with time-dependent source. The dashed lines indicate the minimal error for that particular rank.

a good practical compromise between the two other methods since, as mentioned earlier, it requires only evaluations of φ_1 functions. On the performance figure, it is clear that for a low accuracy, the projected exponential Euler method is faster. For moderate accuracy, one would prefer the non-strict projected exponential Runge; and we recommend using the strict projected exponential Runge for high accuracy.

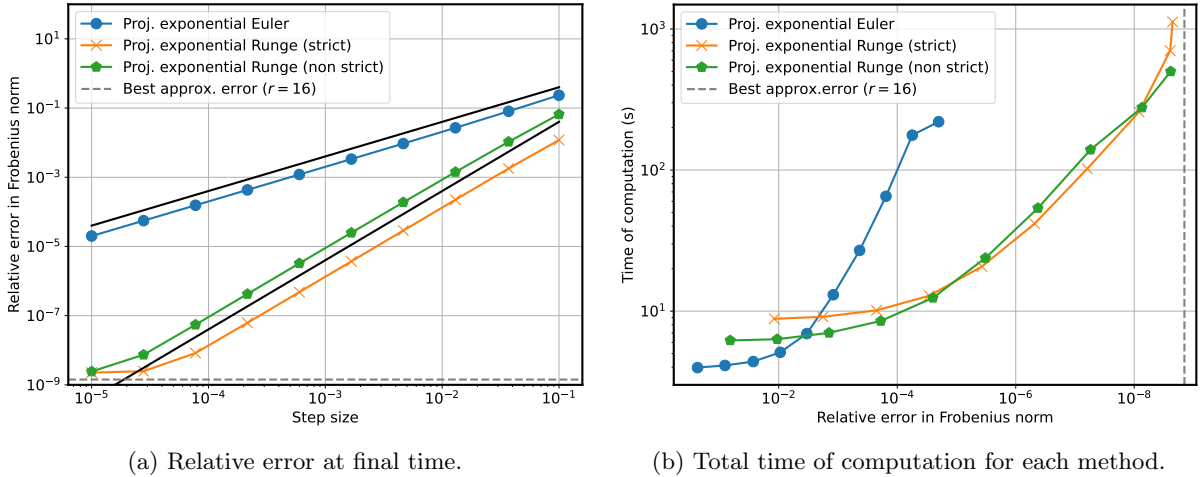


Fig. 4: New methods applied to the differential Lyapunov equation with time-dependent source.

5.2 Application to the differential Riccati equation

In order to compare with existing methods, we consider the problem described in [6] which we briefly restate here. The problem is a differential Riccati equation of the form

$$\dot{X}(t) = A^T X(t) + X(t)A + M^T M - X(t)^2, \quad X(0) = X_0. \quad (54)$$

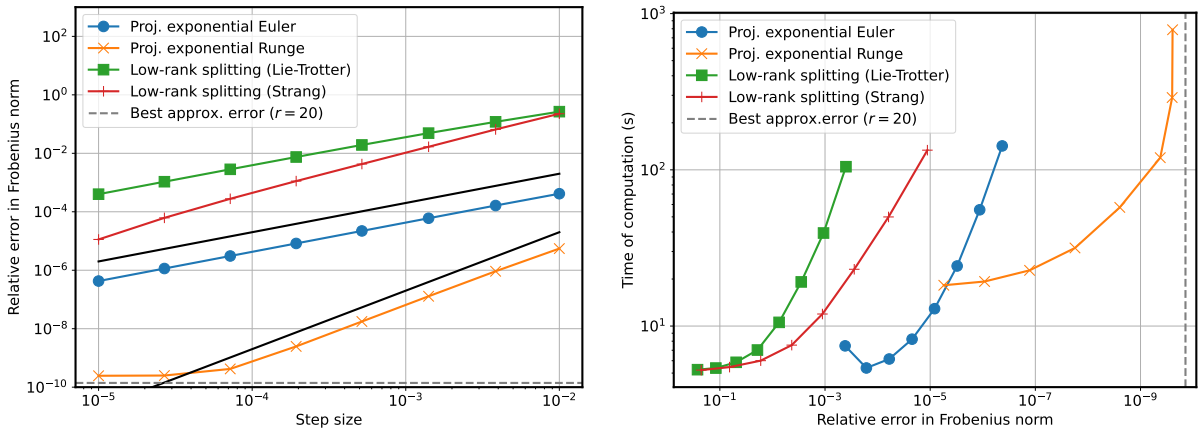
The sparse matrix $A \in \mathbb{R}^{n \times n}$ comes from the spatial discretization of the diffusion operator

$$\mathcal{D} = \partial_x(\alpha(x)\partial_x(\cdot)) - \lambda I, \quad \alpha(x) = 2 + \cos(2\pi x), \quad \lambda = 1,$$

on the domain $\Omega = (0, 1)$ subject to homogeneous Dirichlet boundary conditions. The discretization is done via the finite volume method, as described in [43]. Similarly to before, the constant matrix $M \in \mathbb{R}^{q \times n}$ is defined by taking $q = 9$ independent vectors $\{1, e_1, \dots, e_{(q-1)/2}, f_1, \dots, f_{(q-1)/2}\}$. As initial value, we start from $\tilde{X}_0 = 0$, propagate the solution to time $\delta t = 0.01$ with the reference solver in order to become a physically meaningful initial value X_0 that is full rank. The final time is $T = 0.1$ and the size is $n = 200$. As before, we use extended Krylov spaces with only one iteration. The rank of approximation is $r = 20$.

Comparison with existing methods

Figure 5 shows a comparison between the new methods and the existing methods described in [6]. The figure on the left shows the global error. As we can see, projected exponential Euler and Runge have convergence of order one and two, respectively. That is in agreement with Theorem 10 and Theorem 6. Again, we observe that the new methods have smaller hidden constants compared to existing methods. With enough time steps, the projected exponential Runge method reaches the approximation error which is close to 10^{-10} . On the other hand, the low-rank splitting (Strang) does not show a clear convergence of order two when the step size is too large. We also provide the time of computation on the right figure. For any given accuracy, we can see that the new methods are faster than existing methods.



(a) Global error. The straight black lines are slopes 1 and 2 for visual reference.

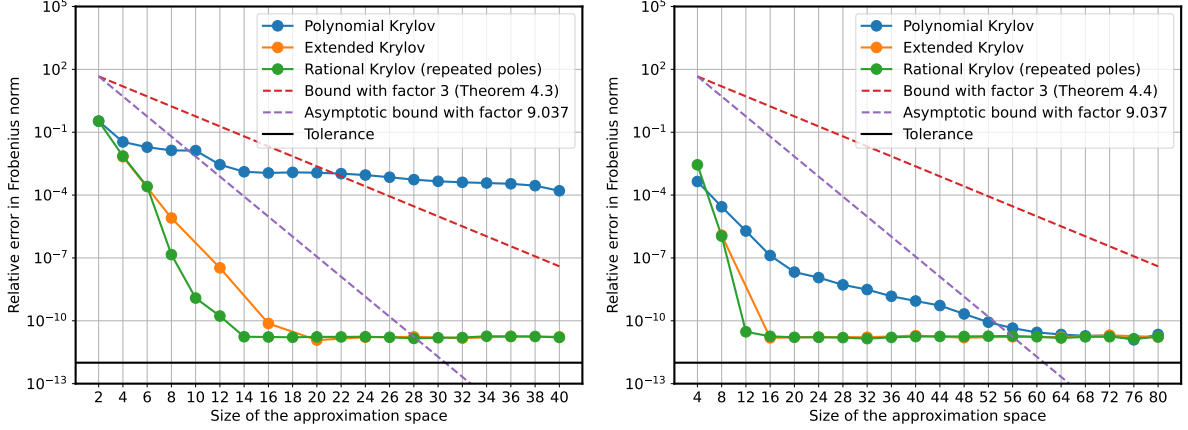
(b) Performance. The dotted line is the approximation error that cannot be outperformed.

Fig. 5: The new methods applied to the differential Riccati equation. The low-rank splitting methods are from [6].

Krylov approximation errors

Let us consider the three different Krylov spaces described in Section 4. Since the spectrum of A is unbounded under mesh refinements, we use a single repeated pole $k/\sqrt{2}$, which turns out to be a simple but already good choice of poles, see [34, Section 4.2]. Strictly speaking, the theoretical bounds derived in Section 4 are only true when optimal poles are used. Nevertheless, the next figure includes the bounds for visual reference.

Figure 6 shows the error made by each type of Krylov space as the size of the space grows, at the time $t = 0.01$. In total, we perform $k = 20$ iterations. We start from the same initial value X_0 truncated to rank 1. Therefore, the approximation space starts from size 2 for the first order approximation, and size 4 for the second order approximation. We deliberately choose a very small rank since it produces clearer convergence plots. In our experiments, a higher rank of approximation always resulted in faster convergence than theoretically predicted. As we can see, in both cases, the rational Krylov shows the faster convergence per iteration. At the opposite, the polynomial Krylov space converges slowly, which implies large dimensional approximation space, and therefore large memory footprint. The extended Krylov space is somewhere in between and seems to be a good practical choice since it avoids the problem of choosing the poles that can be complex numbers (as in the case of optimal poles).



(a) First order approximation: relative errors between the full system (46) and the reduced system (47). (b) Second order approximation: relative errors between the full system (49) and the reduced system (50).

Fig. 6: Approximation error made by the Krylov techniques for reducing an ODE.

5.3 Application to the Allen-Cahn equation

The following example is inspired from [44] and describes the process of phase separation in multi-component alloy systems [45, 46]. In its simplest form, the partial differential equation is given by

$$\frac{\partial f}{\partial t} = \varepsilon \Delta f + f - f^3, \quad (55)$$

where Δf is the diffusion term and $f - f^3$ is the reaction term. The stiffness is controlled with the small parameter ε . Similarly to the paper cited above, we consider the initial condition

$$f_0(x, y) = \frac{\left[e^{-\tan^2(x)} + e^{-\tan^2(y)} \right] \sin(x) \sin(y)}{1 + e^{|\csc(-x/2)|} + e^{|\csc(-y/2)|}}.$$

The space is $\Omega = [0, 2\pi]^2$ and the mesh contains 256×256 points. The time interval is $[0, 10]$. The discretization is done via finite differences, leading to a matrix differential equation of the form

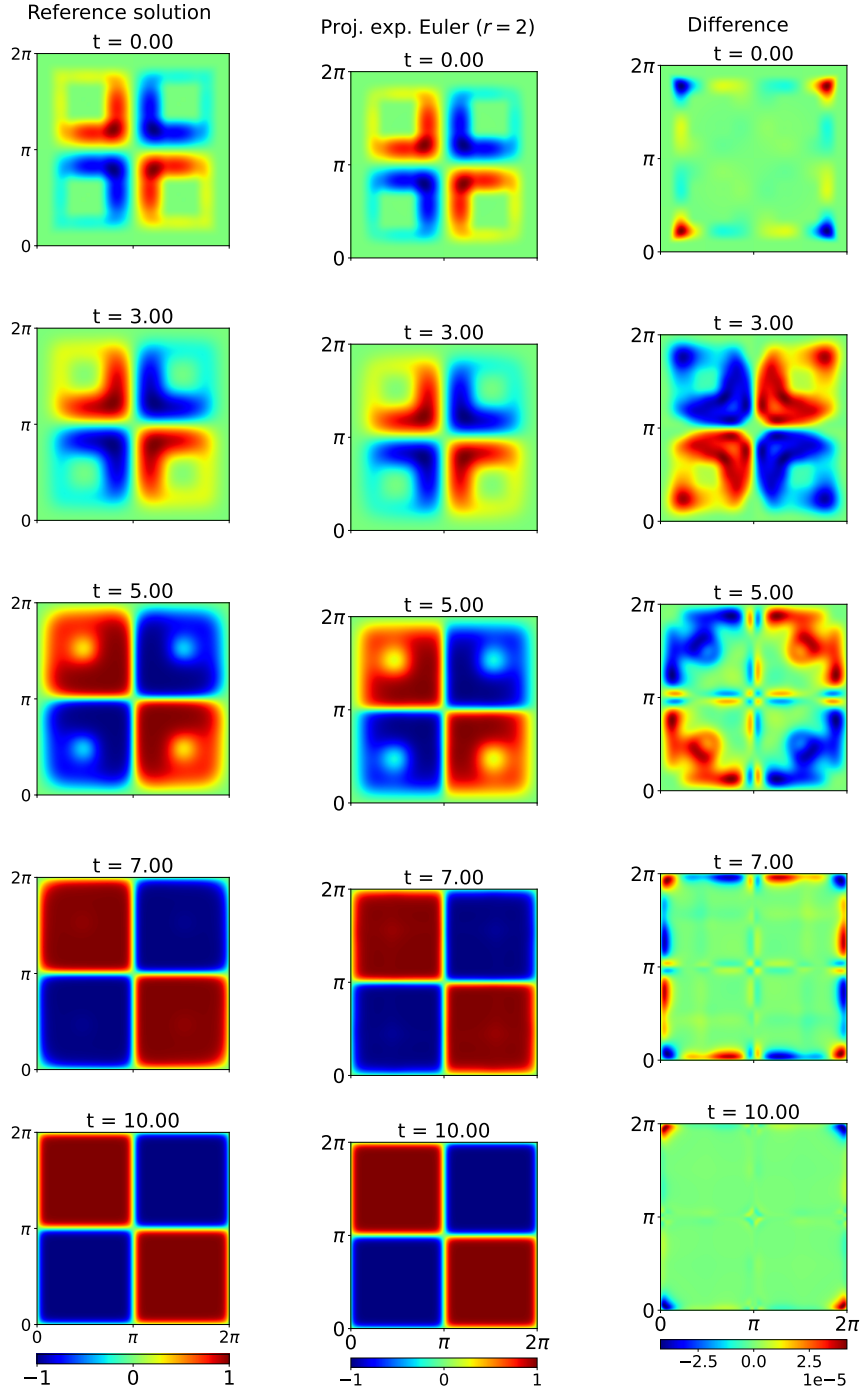
$$\dot{X}(t) = AX(t) + X(t)A + X(t) - X(t)^3, \quad (X_0)_{ij} = f_0(x_i, y_j), \quad (56)$$

where the power is to be taken element-wise ($X^3 = X * X * X$ where $*$ is the Hadamard product). The numerical rank of the initial value is 28. Because of the Hadamard product, the non-linearity is clearly more challenging than in the Lyapunov and Riccati differential equations. A method for performing efficient Hadamard product with low-rank matrices is described in [47], which avoids forming the dense matrix. The growth in rank is therefore limited since $\text{rank}(X^3) \leq \text{rank}(X)^3$. The computations are thus feasible when the rank r is (very) small compared to the size n of the matrix. In this example, we take $r = 2$.

In Figure 7, we give a qualitative comparison between the reference solution and the approximation made by projected exponential Euler. Our method already gives an excellent qualitative approximation despite the small rank $r = 2$. Moreover, the method is significantly faster than the reference solver, which here is scipy's solver RK45 with default tolerance (10^{-8}).

5.4 Rank-adaptive methods

Often in practice, the rank of approximation is not known a priori. In such a situation, we would like to give a tolerance and let the algorithm choose automatically the appropriate rank at each time step. Such methods are called rank-adaptive, and several of them have already been proposed, see [48], [49].



(a) Comput. time: $\approx 5.26s$. (b) Comput. time: $\approx 0.22s$. (c) Normalized error.

Fig. 7: Solution to Allen-Cahn equation (56) at several time points. The reference solution is computed with scipy's default method RK45. The computation time is the total time of computation for all steps. The projected exponential Euler method give excellent qualitative prediction and is significantly cheaper.

Fortunately, the techniques proposed in this paper are easy to transform into rank-adaptive techniques. Indeed, each truncation can be performed at any given tolerance instead of a fixed rank. For example, the adaptive version of projected exponential Euler is given by the iteration

$$Y_1^{\text{APE}} = \mathcal{T}_\tau \left(e^{h\mathcal{L}} Y_0 + h\varphi_1(h\mathcal{L}) \mathcal{P}_{Y_0} [\mathcal{G}(Y_0)] \right),$$

where \mathcal{T}_τ is the truncated SVD up to tolerance τ . It naturally extends to any higher-order scheme.

Let us consider again the Lyapunov differential equation (52) with a time-dependent source. In order to verify the capabilities of the method, we choose a time-dependent source that will modify the singular values significantly so that the ideal rank for a given tolerance is often changing:

$$C(t) = \begin{cases} AX_1 + X_1A^T, & \text{if } 0 \leq t < 0.2, \\ AX_1 + X_1A^T + (t - 0.2)/0.2 \cdot (AX_2 + X_2A^T - AX_1 + X_1A^T), & \text{if } 0.2 \leq t < 0.4, \\ AX_2 + X_2A^T, & \text{if } 0.4 \leq t < 0.6, \\ AX_2 + X_2A^T + (t - 0.6)/0.2 \cdot (AX_1 + X_1A^T - AX_2 + X_2A^T), & \text{if } 0.6 \leq t < 0.8, \\ AX_1 + X_1A^T, & \text{if } 0.8 \leq t \leq 1, \end{cases}$$

where $X_1 = Q\Sigma_1Q^T$ and $X_2 = Q\Sigma_2Q^T$ with singular values $\Sigma_1 = \text{diag}(1, 10^{-2}, 10^{-4}, \dots, 10^{-12}, 10^{-14})$, $\Sigma_2 = \text{diag}(1, 10^{-1}, 10^{-2}, \dots, 10^{-7}, 10^{-8})$ and random $Q \in \mathbb{R}^{n \times 9}$ with orthonormal columns. As we can see in Figure 8, the singular values of the reference solution have essentially five phases, one for each time interval.

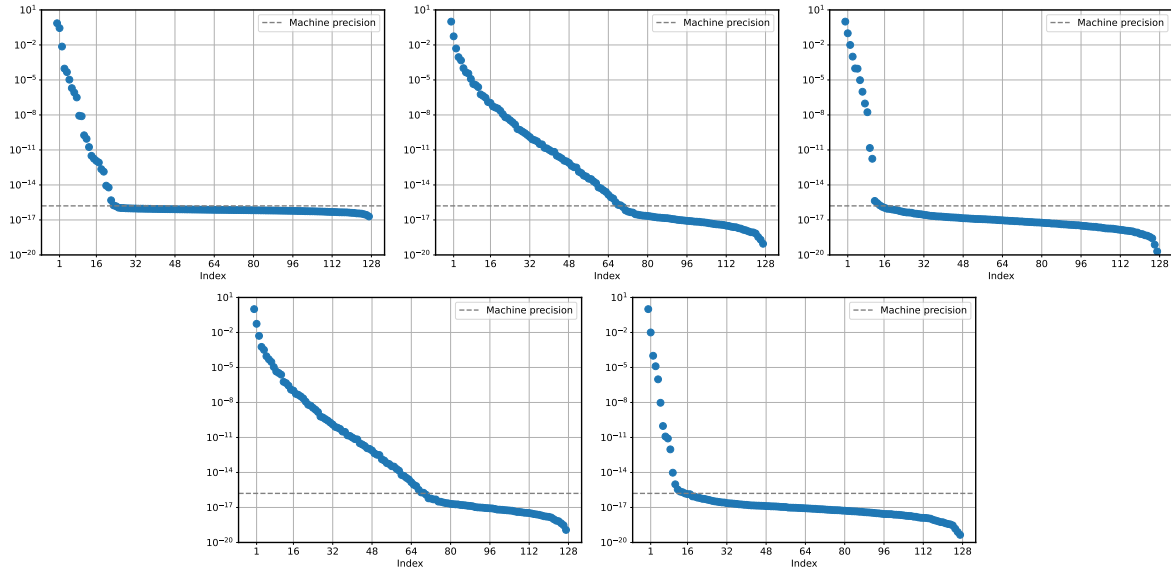


Fig. 8: Singular values of the reference solution at several time points.

In Figure 9, we applied the rank-adaptive projected exponential Runge method with three different tolerances. The step size is $h = 0.001$, and we again used extended Krylov spaces with one iteration. As we can see, the method is able to rapidly adapt the rank, and the small tolerances are able to capture the five phases of the singular values. The peaks in the errors are most likely due to the discontinuous nature of the problem. The relative errors are close to the given tolerances as it should be. Overall, the adaptive methods show good results with no extra cost due to the adaptive rank.

6 Conclusion and future works

In a nutshell, we proposed a new class of methods for the dynamical low-rank approximation that we called projected exponential methods. In particular, we focused on two methods, namely projected exponential Euler and Runge, which we have proven to be robust-to-stiffness with a stiff order one and two, respectively, up to the modelling error due to low-rank. In addition, we described a third, intermediate, technique that only requires evaluating φ_1 functions and that has good practical convergence properties. In order to apply the schemes, we proposed Krylov techniques for efficient implementation, reducing the memory footprint and accelerating the computations. Those techniques are also theoretically analyzed,

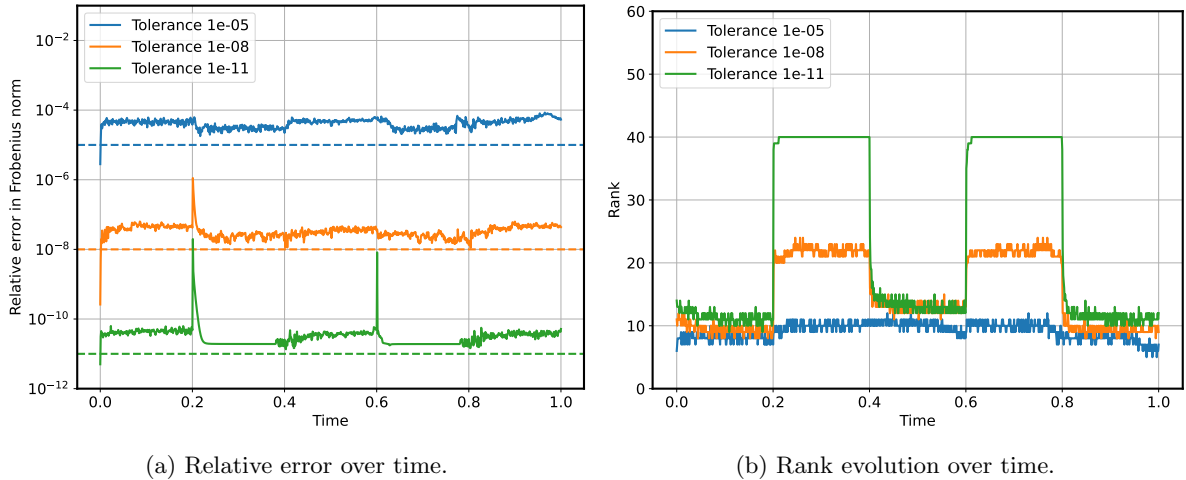


Fig. 9: Adaptive projected exponential Runge applied to the Lyapunov differential equation with time-dependent source. Step size $h = 0.001$.

leading to convergence bounds that can be a guide when choosing the size of the approximation space. Finally, numerical experiments verify the theoretical derivations and show the good performance of the new methods.

An obvious future work is to extend the analysis to higher-order methods. However, higher-order methods will require a significantly larger approximation space, making the computations not feasible in most cases. Recently, many efforts are made into developing iterative methods that are low-rank compatible. It is possible that higher-order projected exponential methods become viable in the near future.

Another possible work would be to extend the framework to dynamical tensor approximation [50]. Certain discretized high-dimensional Schrödinger equations that are stiff are numerically challenging to solve in a large-scale setting. Interestingly, the equation has the structure required for projected exponential integrators, and is therefore a good motivation for studying further those methods in high dimensions.

References

- [1] Koch, O., Lubich, C.: Dynamical low-rank approximation. *SIAM Journal on Matrix Analysis and Applications* **29**(2), 434–454 (2007)
- [2] Lubich, C., Oseledets, I.V.: A projector-splitting integrator for dynamical low-rank approximation. *BIT Numerical Mathematics* **54**(1), 171–188 (2014)
- [3] Ceruti, G., Lubich, C.: An unconventional robust integrator for dynamical low-rank approximation. *BIT Numerical Mathematics* **62**(1), 23–44 (2022)
- [4] Kieri, E., Lubich, C., Walach, H.: Discretized dynamical low-rank approximation in the presence of small singular values. *SIAM Journal on Numerical Analysis* **54**(2), 1020–1038 (2016)
- [5] Hochbruck, M., Ostermann, A.: Exponential integrators. *Acta Numerica* **19**, 209–286 (2010)
- [6] Ostermann, A., Piazzola, C., Walach, H.: Convergence of a low-rank lie–trotter splitting for stiff matrix differential equations. *SIAM Journal on Numerical Analysis* **57**(4), 1947–1966 (2019)
- [7] Horn, R., Johnson, C.R.: *Topics in Matrix Analysis*. Cambridge University Press, Cambridge, UK (1991)
- [8] Skaflestad, B., Wright, W.M.: The scaling and modified squaring method for matrix functions related

- to the exponential. *Applied Numerical Mathematics* **59**(3-4), 783–799 (2009)
- [9] Göckler, T., Grimm, V.: Uniform approximation of φ -functions in exponential integrators by a rational Krylov subspace method with simple poles. *SIAM Journal on Matrix Analysis and Applications* **35**(4), 1467–1489 (2014)
- [10] Hairer, E., Nørsett, S.P., Wanner, G., et al.: Solving ordinary differential equations i [electronic resource]: Nonstiff problems
- [11] Hochbruck, M., Ostermann, A.: Explicit exponential runge–kutta methods for semilinear parabolic problems. *SIAM Journal on Numerical Analysis* **43**(3), 1069–1090 (2005)
- [12] Luan, V.T., Ostermann, A.: Exponential b-series: The stiff case. *SIAM Journal on Numerical Analysis* **51**(6), 3431–3445 (2013)
- [13] Luan, V.T., Ostermann, A.: Stiff order conditions for exponential runge–kutta methods of order five. In: *Modeling, Simulation and Optimization of Complex Processes-HPSC 2012: Proceedings of the Fifth International Conference on High Performance Scientific Computing, March 5-9, 2012, Hanoi, Vietnam*, pp. 133–143 (2014). Springer
- [14] Uschmajew, A., Vandereycken, B.: *Geometric Methods on Low-rank Matrix and Tensor Manifolds*. Springer (2020)
- [15] Hackbusch, W.: New estimates for the recursive low-rank truncation of block-structured matrices. *Numerische Mathematik* **132**(2), 303–328 (2016)
- [16] Gallopoulos, E., Saad, Y.: Efficient solution of parabolic equations by Krylov approximation methods. *SIAM journal on scientific and statistical computing* **13**(5), 1236–1264 (1992)
- [17] Hochbruck, M., Lubich, C.: On Krylov subspace approximations to the matrix exponential operator. *SIAM Journal on Numerical Analysis* **34**(5), 1911–1925 (1997)
- [18] Niesen, J., Wright, W.: A Krylov subspace algorithm for evaluating the φ -functions in exponential integrators. arXiv preprint arXiv:0907.4631 (2009)
- [19] Göckler, T.: Rational Krylov subspace methods for ϕ -functions in exponential integrators. PhD thesis, PhD thesis, Karlsruhe Institute of Technology (KIT), Germany (2014)
- [20] Gaudreault, S., Rainwater, G., Tokman, M.: KIOPS: A fast adaptive Krylov subspace solver for exponential integrators. *Journal of Computational Physics* **372**, 236–255 (2018)
- [21] Botchev, M.A., Knizhnerman, L.A.: Art: Adaptive residual-time restarting for Krylov subspace matrix exponential evaluations. *Journal of Computational and Applied Mathematics* **364**, 112311 (2020)
- [22] Sidje, R.B.: Expokit: A software package for computing matrix exponentials. *ACM Transactions on Mathematical Software (TOMS)* **24**(1), 130–156 (1998)
- [23] Beckermann, B., Güttel, S., Vandebril, R.: On the convergence of rational ritz values. *SIAM Journal on Matrix Analysis and Applications* **31**(4), 1740–1774 (2010)
- [24] Elsworth, S., Guttel, S.: The block rational arnoldi method. *SIAM Journal on Matrix Analysis and Applications* **41**(2), 365–388 (2020)
- [25] Ruhe, A.: The rational Krylov algorithm for nonsymmetric eigenvalue problems. iii: Complex shifts for real matrices. *BIT Numerical Mathematics* **34**, 165–176 (1994)
- [26] Ruhe, A.: Rational Krylov: A practical algorithm for large sparse nonsymmetric matrix pencils.

- SIAM Journal on Scientific Computing **19**(5), 1535–1551 (1998)
- [27] Wilkinson, J.H.: The Algebraic Eigenvalue Problem vol. 662. Oxford Clarendon (1965)
- [28] Al-Mohy, A.H., Higham, N.J.: Computing the action of the matrix exponential, with an application to exponential integrators. SIAM journal on scientific computing **33**(2), 488–511 (2011)
- [29] Simoncini, V.: A new iterative method for solving large-scale lyapunov matrix equations. SIAM Journal on Scientific Computing **29**(3), 1268–1288 (2007)
- [30] Simoncini, V.: Computational methods for linear matrix equations. siam REVIEW **58**(3), 377–441 (2016)
- [31] Behr, M., Benner, P., Heiland, J.: Solution formulas for differential sylvester and lyapunov equations. Calcolo **56**(4), 51 (2019)
- [32] Koskela, A., Mena, H.: Analysis of Krylov subspace approximation to large scale differential riccati equations. arXiv preprint arXiv:1705.07507 (2017)
- [33] Berljafa, M., Elsworth, S., Güttel, S.: A rational krylov toolbox for matlab (2014)
- [34] Güttel, S.: Rational krylov approximation of matrix functions: Numerical methods and optimal pole selection. GAMM-Mitteilungen **36**(1), 8–31 (2013)
- [35] Beckermann, B., Cortinovis, A., Kressner, D., Schweitzer, M.: Low-rank updates of matrix functions ii: Rational krylov methods. SIAM Journal on Numerical Analysis **59**(3), 1325–1347 (2021)
- [36] Petrushev, P.P., Popov, V.A.: Rational Approximation of Real Functions vol. 28. Cambridge University Press (2011)
- [37] Varga, R.S., Ruttan, A., Karpenter, A.: Numerical results on best uniform rational approximation of on. Mathematics of the USSR-Sbornik **74**(2), 271 (1993)
- [38] Al-Mohy, A.H., Higham, N.J.: A new scaling and squaring algorithm for the matrix exponential. SIAM Journal on Matrix Analysis and Applications **31**(3), 970–989 (2010)
- [39] Bartels, R.H., Stewart, G.W.: Solution of the matrix equation $ax + xb = c$ [f4]. Communications of the ACM **15**(9), 820–826 (1972)
- [40] Amato, F., Ambrosino, R., Ariola, M., Cosentino, C., De Tommasi, G., *et al.*: Finite-time Stability and Control vol. 453. Springer (2014)
- [41] Locatelli, A., Sieniutycz, S.: Optimal control: An introduction. Appl. Mech. Rev. **55**(3), 48–49 (2002)
- [42] Carrel, B., Gander, M.J., Vandereycken, B.: Low-rank parareal: a low-rank parallel-in-time integrator. BIT Numerical Mathematics **63**(1), 13 (2023)
- [43] Gander, M.J., Kwok, F.: Numerical Analysis of Partial Differential Equations Using Maple and MATLAB. SIAM (2018)
- [44] Rodgers, A., Venturi, D.: Implicit integration of nonlinear evolution equations on tensor manifolds. Journal of Scientific Computing **97**(2), 33 (2023)
- [45] Allen, S.M., Cahn, J.W.: Ground state structures in ordered binary alloys with second neighbor interactions. Acta Metallurgica **20**(3), 423–433 (1972)
- [46] Allen, S.M., Cahn, J.W.: A correction to the ground state of fcc binary ordered alloys with first and second neighbor pairwise interactions. Scripta Metallurgica **7**(12), 1261–1264 (1973)

- [47] Kressner, D., Perisa, L.: Recompression of hadamard products of tensors in tucker format. *SIAM Journal on Scientific Computing* **39**(5), 1879–1902 (2017)
- [48] Ceruti, G., Kusch, J., Lubich, C.: A rank-adaptive robust integrator for dynamical low-rank approximation. *BIT Numerical Mathematics* **62**(4), 1149–1174 (2022)
- [49] Hochbruck, M., Neher, M., Schrammer, S.: Rank-adaptive dynamical low-rank integrators for first-order and second-order matrix differential equations. *BIT Numerical Mathematics* **63**(1), 9 (2023)
- [50] Koch, O., Lubich, C.: Dynamical tensor approximation. *SIAM Journal on Matrix Analysis and Applications* **31**(5), 2360–2375 (2010)

A Convergence proof of exponential Euler

The following is the proof of Theorem 4.

Proof. Let us start with a Taylor expansion of the closed form solution:

$$\begin{aligned} X(t_n) &= e^{h\mathcal{L}}X(t_n) + \int_0^h e^{(h-\tau)\mathcal{L}}f(t_n + \tau)d\tau \\ &= e^{h\mathcal{L}}X(t_n) + h\varphi_1(h\mathcal{L})f(t_n) + \int_0^h e^{(h-\tau)\mathcal{L}} \int_0^\tau f'(t_n + \sigma)d\sigma d\tau. \end{aligned}$$

Therefore, the error $E_{n+1} = X_{n+1}^E - X(t_{n+1})$ verifies the following recursion:

$$E_{n+1} = e^{h\mathcal{L}}E_n + h\varphi_1(h\mathcal{L})[\mathcal{G}(X_n) - f(t_n)] - \delta_{n+1},$$

where δ_{n+1} is the remainder term at the step $n + 1$. Taking the norm and using the Lipschitz continuity of \mathcal{G} gives that

$$\|E_{n+1}\| \leq e^{h\ell} \|E_n\| + h \cdot \varphi_1(h\ell)L_G \cdot \|E_n\| + \|\delta_{n+1}\|$$

which leads to

$$\|E_{n+1}\| \leq (1 + hL_*) \|E_n\| + \|\delta_{n+1}\|,$$

where $L_* = \ell + \varphi_1(h\ell)L_G$. The remainder term is bounded by

$$\begin{aligned} \|\delta_{n+1}\| &\leq \int_0^h e^{(h-\tau)\ell} \tau d\tau \max_{0 \leq s \leq h} \|f'(t_n + s)\| \\ &\leq h^2 \varphi_2(h\ell) \max_{0 \leq s \leq h} \|f'(t_n + s)\| \\ &\leq h^2 \varphi_2(h\ell) \max_{0 \leq s \leq t_{n+1}} \|f'(s)\| = h\beta. \end{aligned}$$

Solving the recursion as done in (24) leads to

$$\|X_n - X(t_n)\| \leq \frac{e^{nhL_*} - 1}{L_*} \cdot \varphi_2(h\ell) \cdot \max_{0 \leq t \leq t_n} \|f'(t)\|.$$

For all $h \leq h_0$ small enough, the factors above reduce to a constant $C(\ell, L_G, h_0)$ as stated in the theorem. \square